

## Review Article

# Raman Spectroscopy for Clinical Oncology

**Michael B. Fenn,<sup>1,2</sup> Petros Xanthopoulos,<sup>3</sup> Georgios Pyrgiotakis,<sup>2,4</sup>  
Stephen R. Grobmyer,<sup>5</sup> Panos M. Pardalos,<sup>3,6,7</sup> and Larry L. Hench<sup>8</sup>**

<sup>1</sup> Department of Materials Science and Engineering, University of Florida, Particle Science and Technology Building, 205 Center Drive, P.O. Box 116595, Gainesville, FL 32611, USA

<sup>2</sup> Particle Engineering Research Center, University of Florida, Particle Science and Technology Building, 205 Center Drive, P.O. Box 116595, Gainesville, FL 32611, USA

<sup>3</sup> Department of Industrial and Systems Engineering, University of Florida, 303 Weil Hall, P.O. Box 116595, Gainesville, FL 32611-6595, USA

<sup>4</sup> Department of Environmental Health, Harvard School of Public Health, 677 Huntington Avenue, Boston, MA 02115, USA

<sup>5</sup> Division of Surgical Oncology, Department of Surgery, College of Medicine, University of Florida, P.O. Box 100286, Shands Hospital, 1600 Archer Road, Gainesville, FL 32610, USA

<sup>6</sup> Crayton Pruitt Family Department of Biomedical Engineering, University of Florida, Gainesville, FL, USA

<sup>7</sup> McKnight Brain Institute, University of Florida, 303 Weil Hall, P.O. Box 116595, Gainesville, FL 32611-6595, USA

<sup>8</sup> Department of Materials Science and Engineering, University of Florida, 100 Rhines Hall, P.O. Box 116400, Gainesville, FL 32611-6400, USA

Correspondence should be addressed to Michael B. Fenn, mfenn@perc.ufl.edu

Received 31 May 2011; Revised 9 August 2011; Accepted 11 August 2011

Academic Editor: Ci-Ling Pan

Copyright © 2011 Michael B. Fenn et al. This is an open access article distributed under the Creative Commons Attribution License, which permits unrestricted use, distribution, and reproduction in any medium, provided the original work is properly cited.

Cancer is one of the leading causes of death throughout the world. Advancements in early and improved diagnosis could help prevent a significant number of these deaths. Raman spectroscopy is a vibrational spectroscopic technique which has received considerable attention recently with regards to applications in clinical oncology. Raman spectroscopy has the potential not only to improve diagnosis of cancer but also to advance the treatment of cancer. A number of studies have investigated Raman spectroscopy for its potential to improve diagnosis and treatment of a wide variety of cancers. In this paper the most recent advances in dispersive Raman spectroscopy, which have demonstrated promising leads to real world application for clinical oncology are reviewed. The application of Raman spectroscopy to breast, brain, skin, cervical, gastrointestinal, oral, and lung cancers is reviewed as well as a special focus on the data analysis techniques, which have been employed in the studies.

## 1. Introduction

Cancer continues to persist as one of the most common causes of death throughout the world and remains the second leading cause of death in the United States [1]. This rise in cost coincides with estimates that 1,529,560 new cases of cancer were diagnosed, and 569,490 cancer-related deaths had occurred in 2010 in the US alone [2]. There has been some slight progress recently with recent studies showing a decrease in cancer incidence of 1.7% during the recent period of 2001–2005; and some cancers such as breast cancer have shown a reduction in cancer related mortality

over the last 10 years. However, much more progress is needed to improve diagnosis and treatment of cancer in order to ultimately reduce cancer-related suffering and death. Research for cancer diagnosis and treatment has continued to yield advances in chemotherapy regimens, radiation therapy, surgical procedures, and imaging technologies. Biomedical imaging modalities such as magnetic resonance imaging (MRI), positron emission tomography (PET), and computed tomography (CT) for cancer diagnosis have progressed significantly in recent decades [3]. Using these imaging modalities, surgeons have been able to perform surgical procedures with greatly improved accuracy in location of

lesions and adjacent anatomical structures yielding better outcomes. However, these conventional modalities have drawbacks, particularly in regards to intraoperative use. Thus, current research has presented an increasing focus on the biomedical applications of optical imaging technologies, known as biophotonics, for clinical applications in oncology. Offering the surgeon technologies, which could allow real-time imaging for intraoperative identification of tissues and even cells, could potentially have a profound effect on surgical outcomes, staging, and adjuvant therapy regimens. Such image-guided surgical technologies could afford the surgeon the ability to demarcate tumor margins with an exceptionally high degree of accuracy and remove premalignant or microscopic metastases which previously would have been missed.

Optical technologies are also being heavily investigated for use in the pathology laboratory for the evaluation of excised tissues such as biopsies of potentially cancerous lesions. Currently, the gold-standard for assessing adequate margin clearance or tissue malignancy is biopsy, followed by histopathological evaluation. Examination of the tissue for intraoperative biopsy is typically completed by one of two techniques, imprint cytology or frozen sectioning. Numerous other molecular-based test platforms do exist, although they are less commonly used. Most frequently the tissues samples are obtained, formalin-fixed, paraffin-embedded, and sectioned for hematoxylin and eosin (H&E) staining, and sometimes immunohistochemical assay. These procedures are not only time consuming but also expensive. The methods of histopathological analysis currently in routine use for investigating suspected cancerous or pre-cancerous lesions have several disadvantages. One of the most prominent of these disadvantages is the error associated with subjectivity which can be introduced by intraobserver variation when visually evaluating tissue sections. Furthermore, the extended surgical time needed to obtain pathology results puts the patient at greater risk due to prolonged exposure to general anesthesia. It should also be noted that variation in the technique used from center to center potentially hinders the comparison of clinical outcomes. Finally, the need to have a trained pathologist examine each biopsy further increases the expense of an already costly procedure. Therefore, more rapid, objective technologies are needed, which optimally could be executed in the operating suite by the surgeon. Recently, optical imaging technologies have been under investigation for improving cancer diagnosis and treatment, as they can provide rapid, real-time tissue evaluation with a high degree of spatial resolution [3]. Raman spectroscopy has demonstrated several major advantages over other optical techniques and may hold promise for improving cancer diagnosis and treatment outcomes in the future.

Recent advances in Raman spectroscopy have given way to a wide range of biomedical applications including cancer. Its ability to detect variance related to DNA/RNA, proteins, and lipids have made it an excellent tool for quantifying changes on the cellular level, as well as differentiating between various cell and tissue types. Figure 1 shows an example of a Raman spectrum with regions specific to the

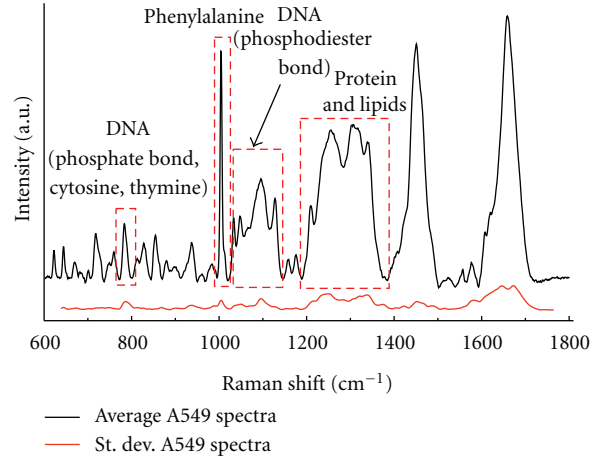


FIGURE 1: Example of an average Raman spectrum from a lung cancer cell (black) after baseline subtraction. The major spectral peaks and regions which correlate to the molecular vibrations collected from Raman scattering of DNA, lipids, and proteins are highlighted. (Note that the  $x$ -axis is in Raman shift which is defined in wavenumber ( $\text{cm}^{-1}$ ), the inverse of wavelength in centimeters).

various biomolecules highlighted. Changes in these regions amongst spectra collected from one tissue, or tissue region, to another allow for differentiation or classification of the tissues based on their corresponding spectra. The presence or lack of spectral regions, or specific peaks, can be correlated to differences in biochemical composition between cells and tissues. Due to the complexity of the spectra and the large amount of data contained within the spectra, various statistical methods can be employed to allow for data analysis and extraction.

The collection of Raman spectra from biological samples produces a “fingerprint” representing the molecular vibrations specific to chemical bonds, thus yielding information of a samples chemical (or biochemical) composition. The Raman “fingerprint region”, between  $500$  and  $2000 \text{ cm}^{-1}$ , is the region of the Raman spectrum, which correlates to the molecular vibrations of biochemical importance. The collection of spectra can be performed *in vitro*, *ex vivo* or *in vivo* without disrupting the cellular environment. This is a major advantage of Raman spectroscopy, as most biological assays utilize chemical biomarkers and often require conditions nonnative to the biological environment. A typical Raman instrument for biomedical applications will employ a near-infrared (NIR) laser, often a diode laser, which has a very narrow excitation wavelength in the optimal range of the NIR for collecting scattered light of interest from biological samples. Figure 2 shows a typical setup for a dispersive Raman spectrometer attached to a microscope, sometimes referred to as micro-Raman spectroscopy. The NIR laser provides a greatly reduced background autofluorescence and absorbance, which are usually problematic when cells and tissues are irradiated at visible or ultraviolet wavelengths. Raman spectroscopy also yields a very low signal from water in the fingerprint region, which makes it advantageous over other infrared techniques such as Fourier-transform infrared

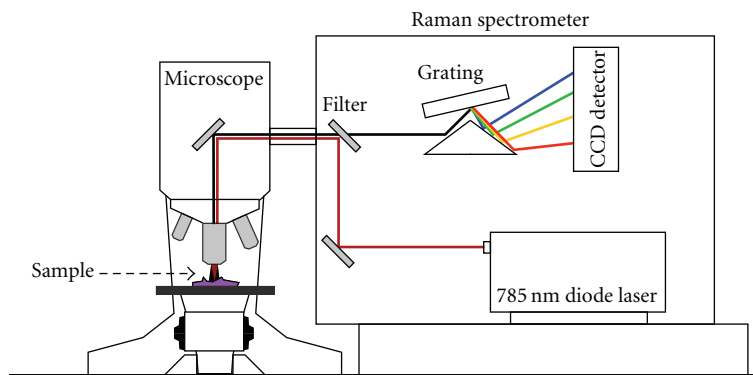


FIGURE 2: Typical setup for a Raman spectrometer with a near-infrared laser attached to a microscope.

spectroscopy (FTIR). It has also been demonstrated that cell survival is not affected by exposure to the Raman laser, even after extended periods of exposure to the relatively low power laser light typically used for dispersive NIR Raman spectroscopy [4]. Raman has been shown to be an effective tool for examining toxicological effects of various materials, cell differentiation, cell proliferation on tissue engineering constructs, material biocompatibility, pharmacological efficacy, and determining cell death mechanisms [5–10]. Clinical applications of Raman spectroscopy are currently in the developmental stages, ranging from the laboratory bench-top to the patient's bedside [11].

The datasets obtained from the collection of Raman spectra from biological samples are massive and the single spectrum peak patterns add an additional level of complexity. Discerning meaningful differences between spectra and regions of interest within spectra require the use of powerful mathematical techniques to allow for the complete extraction and correlation of the data. As the applications of Raman spectroscopy increase in intricacy so does the complexity of datasets and the computational power required for data analysis. Thus one of the primary areas of interest in regards to moving Raman spectroscopy to clinical application is the development of appropriate data processing methods. The combination of advanced data mining techniques with biomedical Raman spectroscopic instruments could allow for rapid, accurate classification and mapping of tissue in the clinical setting. The implementation of advanced data mining techniques based on machine learning may be able to provide the necessary real-time discrimination between normal and cancerous tissues. Furthermore, employing feature selection algorithms could provide real-time immunohistochemical information, which by conventional means is not currently possible. Development of a fully functional Raman instrument could reduce operating time and potentially provide more reliable information than conventional histopathological techniques. Thus, a Raman spectroscopic system could decrease the cost of surgical procedures and most importantly improve the clinical outcome for the patient.

Recent advances in the field of Raman spectroscopy for biomedical applications have been emerging at a rapid pace.

Research has continued to focus on the development of both instrumentation and data analysis techniques. This paper is an attempt to synthesize the literature which forms the basis for the major areas of development towards clinical applications of dispersive Raman spectroscopy in recent years. Other variations of Raman spectroscopy are also currently being investigated for clinical application and have been reviewed elsewhere (see [12]). Applications of Raman spectroscopy for cancers of the breast, brain, gastrointestinal tract, cervix, skin, lungs, and mouth are discussed in the subsequent sections. The following section is dedicated to reviewing some of the common trends in data analysis of Raman spectra, as well as to provide some basic working definitions of these concepts which are employed throughout the literature.

## 2. Data Analysis for Biomedical Applications of Raman Spectroscopy

In order to bridge the gap between the laboratory and patient care for applications of Raman spectroscopy, both hardware and software technologies must be appropriately developed so as to exceed the performance of current technologies. This section provides a brief discussion of some of the commonly applied data analysis techniques, which in the future may provide the basis for software applications incorporated within clinical Raman spectroscopic instrumentation. Analysis of Raman spectroscopic data can be a time-consuming and tedious task using traditional techniques which require peak deconvolution and statistical analysis of the fitted peaks. Such peak analysis methods are prone to error as peak positions are selected manually prior to deconvolution. To improve information extraction from Raman data, more sophisticated data analysis and data mining techniques have been employed with an emphasis placed on supervised learning methods such as linear and nonlinear classifiers. Furthermore; in order to improve the accuracy of such methods feature selection preprocessing can be applied. The aim of such preprocessing steps is to improve data analysis whereas at the same time allow for identification of the spectral regions, which play an important role in the differentiation and classification schemes.

For most biological applications of Raman spectroscopy, particularly those performed *in vivo*, spectral data sets are typically vast and significant spectral features can be difficult, if not impossible, to discern manually. As research of Raman spectroscopy continues to move towards clinical applications, successful translation of this technology will rely in part upon the development of data analysis techniques, which are both highly accurate and rapid. In the clinical setting, real-time data analysis is critical as many Raman spectroscopic applications have been proposed for intraoperative use, such as providing *in situ* classification for diagnosis or imaging of tissues. To achieve, and even surpass, these requirements of speed and accuracy many researchers have been adopting alternative data analysis techniques that are based on statistical machine learning and optimization. Among the emerging and most commonly employed techniques are Principal Component Analysis (PCA) [13], Fisher's Linear Discriminant Analysis (LDA) [14], and more recently supervised learning techniques such as Support Vector Machines (SVM) [15]. Other techniques have also been employed such as artificial neural networks for classification as well as various regression techniques for feature extraction of diagnostically significant peaks and spectral regions. Often combinations of these techniques may be employed to improve accuracy and robustness of the algorithms. Preprocessing techniques such as filtering and evaluation methods such as k-fold cross validation are also often used to achieve even greater accuracy. Having an understanding of these techniques is advantageous as the translational process of Raman spectroscopy to the clinic progresses. The following provides a brief introduction to several of the most prospective techniques. Table 1 provides an example of the several methods of data analysis applied to different cancers, serving to demonstrate the variation across the field. For a more in depth discussion of each technique and its applications the reader is directed to corresponding references.

Throughout the literature, the performance of a binary classification test is quantified by the statistical classification functions: specificity and sensitivity. Overall accuracy is also commonly stated as long as prevalence is known based on sensitivity and specificity. Sensitivity corresponds to the classification algorithm's ability to classify positive results by measuring the proportion of true positives, which are correctly classified as such. Specificity corresponds to the classification algorithm's ability to classify negative results by measuring the proportion of true negatives, which are correctly classified as so. For binary classification algorithms, accuracy is a statistical measure of the proportion of true results in a population. These terms are used frequently in the literature under review herein, thus understanding the definition and concepts of each is important to assess the performance of an algorithm applied to Raman spectroscopy for cancer diagnosis.

Often used in combination, PCA and LDA provide efficient methods for data analysis and visualization of Raman spectroscopic datasets. The PCA transformation is used for reducing the dimensionality of the data (spectra), thus making possible the visualization of cell or tissue

spectra in a low-dimensional space. PCA provides a means to identify patterns in data sets by expressing data in high dimensions and emphasizing the similarities and variances of the data set. PCA by itself is employed by many researchers, mainly because it is a well-studied, traditional statistical method and the results are easily interpretable. Where PCA describes the trends in data, LDA attempts to classify data by maximizing data set separation. LDA maximizes intergroup variance and minimizes intragroup variance to obtain the greatest separation or discrimination between groups. LDA is used in order to identify hyperplanes which maximize the separation between different classes, and thus provide a formal discrimination rule. PCA and LDA have been used in a broad range of applications involving Raman spectroscopy for cancer studies, including gastric cancer [19] and leukemia [20]. Although PCA and LDA are two of the most common methods for classification of Raman spectra, other techniques such as hierarchical cluster analysis [21] and k-means cluster analysis [22] are also found in the literature; examples can be found in [23, 24], respectively.

One of the more recent trends in data analysis for Raman spectroscopy is the use of advanced machine learning techniques for spectral discrimination and interpretation. Supervised learning is one of the most important branches of data mining and is used in many different fields for classification problems. Machine learning consists of an algorithm capable of "learning" from the data by creating an inferred function called a classifier, which can then issue predictions on new data during testing. Supervised learning consists of two main phases: (1) the training phase where the algorithm is trained through a small training set of known examples (e.g., spectra of known healthy and known cancerous cells) and (2) the testing phase where the algorithm calculates which class to group unknown samples (e.g., spectra from cells of unknown type). The fundamental function of the algorithm is to determine a classification rule for some set of data by calculating a hyperplane, or decision rules for classification, that separates the points which belong to two different classes. The hyperplane selected for this task maximizes the margin between the two classes. Figure 3 demonstrates the construction of the hyperplane during the training phase. The hyperplanes are constructed by a set of data with known labels, or in other words, supervised in the learning process. This procedure is repeated many times with different arrangements of training and testing data and every time the overall accuracy is recorded. Such a process is known as cross validation [25]. One of the most common means for evaluating a models accuracy is by using leave-one-out cross validation (LOOCV). When applying LOOCV all but one of the observations is used for training and the remaining observation is tested against the trained model with this procedure repeated for all observations in the set of outputs.

Support vector machines are one of the many types of supervised learning algorithms which have been applied to Raman spectra for classification of cancerous tissues; other algorithms include artificial neural networks, k-nearest neighbor algorithm, and decision tree learning. Originally proposed by Vapnik [26, 27], SVM is one of the most

TABLE 1: A summary demonstrating three different data analysis techniques applied to diagnosis of different types of cancer. The reference for each is presented. This table is purely to show the different applications for each technique and is by no means inclusive of all literature.

Data analysis method	Type of cancer	Number of Patients or spectra collected	Sensitivity	Specificity	Reference
PCA	Brain (neuroblastoma, ganglioneuroma)	698 spectra	100%	100%	[16]
PCA and LDA	Breast	20 patients	92%	100%	[17]
SVM	Breast (axillary lymph nodes)	10447 spectra	100%*	100%*	[18]

\*The SVM used a kernel constructed based on a radial basis function and achieved the highest specificity and sensitivity compared to other kernels.

successful supervised learning methods and has strong mathematical optimization foundations. Apart from being successful in a large number of applications in science and engineering, SVM is preferred also because it is computationally tractable. Existing efficient implementations of SVM allows massive processing of large datasets. Many studies have successfully applied SVM and other supervised learning methods for data analysis of Raman spectra. In the following section, examples are reviewed in which both supervised and unsupervised data analysis techniques are applied.

### 3. Raman Spectroscopy for Diagnosis and Treatment of Cancer

**3.1. Breast Cancer.** There are over 2.5 million women in the United States currently living with breast cancer [28]. Breast cancer is the most common type of cancer in women, excluding skin cancers, and is one of the most deadly in women, second only to lung cancer. The most common type of invasive breast cancer is Infiltrating (or Invasive) Ductal Carcinoma (IDC), accounting for about 80% of all breast cancers [29]. Mammograms or breast ultrasounds are most often the initial indicators of breast cancer, although biopsy of suspicious tissue is the only means to determine if a lesion is benign or cancerous. Several studies have demonstrated that Raman spectroscopy is capable of differentiating cancerous and benign breast lesions from normal tissue by the evaluation of biopsies with high sensitivities and specificities. Haka et al. collected spectra from nine major morphological components of breast tissue to yield a set of basis spectra that were then used to develop a linear combination model, which fits the spectra of native breast tissue [30]. Initially studies employing this model were performed *ex vivo* using excised fresh-frozen biopsy tissue specimens from 58 patients for classification as normal, fibrocystic change, fibroadenoma, or infiltrating carcinoma. It was discovered that the fit coefficients for fat and collagen were of greatest diagnostic significance in the classification model, yielding a specificity and sensitivity of 96% and 94%, respectively. Shortly thereafter, this same group demonstrated the first *in vivo* collection of Raman spectra for breast tissue evaluation; employing the same diagnostic algorithm for intraoperative tumor margin assessment of nine patients undergoing partial mastectomy procedures [31]. Although the data set was small, sensitivities and specificities were perfect (100%) and accuracy was 93.3%. Interestingly, the

Raman spectra from one margin correlated to a cancerous lesion which was grossly invisible, and upon postoperative pathological findings the margin was deemed positive which then required a second operation for excision.

Several other recent studies have been completed in which Raman spectroscopy was used to successfully classify excised breast tissue as cancerous, benign or normal with the results correlating closely to conventional histopathological findings [32–34]. Kumar et al. compared spectra from 69 frozen breast tissue samples collected during surgical resection to a standard set of reference spectra [34]. The reference spectra were constructed in a previous study by employing principal component analysis (PCA) and further model refinement by using Mahalanobis distances and spectral residuals. The standard set of spectra correlated to malignant, benign, and normal breast tissues. Of the 69 tissue samples, 61 of the unknown tissues were classified unambiguously, 29 normal, 17 malignant, and 15 benign. The tissues which did not classify unambiguously against the training set had one or more spectra which classified as diseased, and thus any indication of pathology resulted in the tissue being classified as diseased. Using this classification scheme, strong agreement was observed between the pathology report and the final Raman spectral analysis report. Haka et al. performed a similar study involving a prospective analysis of fresh tissue sections from 21 patients, once more utilizing the algorithm described in [30]. Again, the fit coefficients of fat and collagen were used as key diagnostic factors for distinguishing between the four tissue pathologies [32]. This study by Haka et al. examines the performance of the algorithm and the bias encountered in respect to the different settings of the two studies in which the specimens were collected and analyzed. It also demonstrates the need to fully assess algorithms developed *in vitro* prior to application *ex vivo* or *in vivo* so as to allow for modification and correction in order for accurate diagnostic capability to be achieved.

The severity of breast cancer is highly dependent upon the type and stage of the cancer. Ductal carcinoma in situ (DCIS) is the most common noninvasive breast cancer, typically involving only the ductal walls, and is usually curable by the combination of surgical resection and occasionally adjuvant radiation [2]. Although DCIS is often curable and even sometimes referred to as “stage zero”, the presence of DCIS greatly increases the risk of the patient developing invasive breast cancer [35]. Rehman et al. were able to distinguish between the nuclear grade of DCIS and IDC of specimens from breast cancer patients by describing the

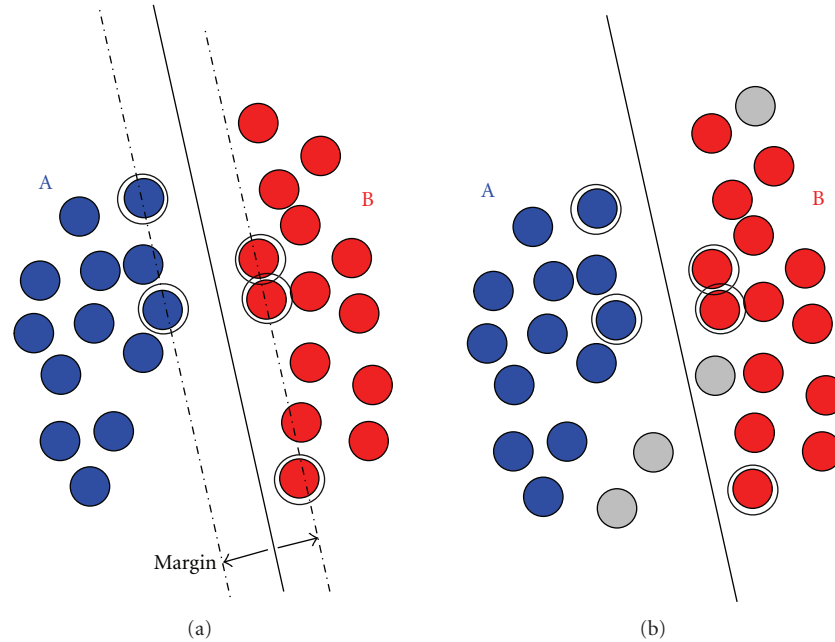


FIGURE 3: All potential hyperplanes are evaluated during the training phase of SVM, and the hyperplane chosen is the one which maximizes the separation margin (a). Once the algorithm is trained based on data with known labels, the hyperplane yields a classification rule which is capable of discriminating samples with unknown labels (training dataset). Unknown data points are represented by gray circles (b).

spectral differences observed [36]. In the Rehman et al. study, 67 breast tissue samples were examined by Raman microspectroscopy. The spectral differences between high, intermediate, and low nuclear-grade DCIS and Grade I–III IDC were described based on peaks and regions of the Raman spectra defined collectively from previous studies. This study shows the potential for Raman spectroscopy in guiding decisions and staging of breast cancer treatment.

The traditional indicator for metastases is based on the histological composition of the axillary lymph nodes and has become the predominant means for staging breast cancers. Histopathological analysis of the sentinel axillary lymph nodes has become a standard procedure prior to complete dissection and removal of the axillary lymphatic drainage [37]. Examination of the biopsy for intraoperative assessment is typically done by conventional histopathological examination. Horsnell and colleagues recently achieved successful differentiation of diseased and normal axillary lymph node biopsies excised and frozen from breast surgeries using simple majority voting in an algorithm based on principal component analysis (PCA) and linear discriminant analysis (LDA) [17]. Spectra were collected from 38 axillary nodes excised from 20 patients. Using a leave-one-out cross validation combined with PCA-LDA, the model achieved a classification sensitivity of 92% and a specificity of 100%. The Raman spectral data was compared to conventional histopathological analysis, and the results were found to strongly agree with one another. To improve data analysis and spectral classification, a necessary requirement for clinical application, Horsnell and colleagues applied support vector machines (SVMs) to Raman spectra from 43 axillary lymph nodes [18]. Three SVM models, based on different

kernels, linear, polynomial, and radial basis function, were developed and compared with traditional models based on linear discriminant analysis and partial least squares discriminant analysis. It was found that the classification improved with the application of an SVM radial basis function model yielding a classification of 100% for testing data. To further improve the data analysis, a preprocessing technique was also applied which implemented filtering. This study demonstrates the benefits which can be achieved by applying advanced data mining techniques such as SVM to the complex and vast data sets acquired from tissues by Raman spectroscopy.

Raman spectroscopy has shown promise for use as a clinical tool for both diagnosis and for use during treatment of breast cancer. Design of a fiber-based probe Raman system with spectral acquisition times and spatial resolution optimized for clinical use is an area which needs further investigation. Studies of larger patient populations will be needed as well. Work has already begun regarding the establishment of spectral markers for breast cancer which can act as pathological indicators similar to that of immunohistochemistry techniques [38]. Relating breast density to the spectral markers such as the spectral signatures related to collagen and fat content may help to incorporate Raman spectroscopy into the arsenal for analysis of biopsied tissue such as fine-needle aspiration (FNA). This may provide a means for not only diagnosis, but risk assessment and monitoring response to risk reduction strategies as well. Improvements on current data analysis techniques, including the application of advanced data mining methods, along with novel preprocessing techniques will also be critical. The application of Raman spectroscopy to the treatment of breast

cancer has thus far shown some of the greatest potential for the emergence of the technology in the clinic.

**3.2. Skin Cancer.** Skin cancer may be subdivided into three distinct types: basal cell carcinoma (BCC), squamous cell carcinoma (SCC), and malignant melanoma (MM). The most common type of skin cancer, as well as the most common malignancy overall in the United States, is nonmelanoma skin cancer (NMSC). The majority of skin cancers are NMSC, which encompasses BCC and SCC, of which over 2 million cases are reported annually [39]. Approximately 80% of all NMSC cases are BCC. Exposure to ultraviolet radiation from the sun is the most common risk factor associated with all skin cancers. Although malignant melanoma is less common than NMSC, approximately 75% of all skin-cancer-related deaths are caused by MM [40]. While BCC and SCC are often cured by simple excision of the lesion, malignant melanoma is often more aggressive and prone to metastasis, thus early detection improves prognosis significantly. Although BCC is often not fatal, it can result in severe disfigurement, and left untreated can spread and result in death. Early detection can improve outcomes, but the ability to identify malignant skin lesions is often dependent upon the training of the physician [41]. Currently, Mohs micrographic surgery is the standard treatment for BCC, which involves successive excision of one layer of skin followed by immediate histopathological examination prior to removal of the subsequent layer [42]. Typically, the histopathology is performed by the dermatologic surgeon, a time- and resource-consuming task [43]. A more efficient method is warranted as the histopathology has associated subjectivity due to interobserver variability even when performed by an experienced histopathologist [44]. Raman spectroscopy could potentially provide a clinical tool which would limit the variance related to the diagnosis of skin neoplasms by providing a more rapid, objective diagnosis based on molecular composition of suspicious skin lesions. The obvious easy access to skin also makes skin a good candidate for diagnosis via Raman spectroscopic analysis.

As the need for a convenient, rapid, and objective means for real-time analysis of suspicious skin lesions has been presented, several groups have investigated the use of Raman spectroscopy for histopathological classification. Lieber et al. developed a portable confocal Raman device with a handheld probe with which spectra from 21 lesions on 19 patients were collected *in vivo* [45]. The collected spectra were then classified as normal, inflamed, BCC, or SCC lesions. The distinction between inflamed tissues of previous surgical excisions from that of recurrent cancerous tissue is of importance to the dermatologist so as to obviate the need for unnecessary additional surgical procedures. The spectra collected from the 21 lesions were processed qualitatively using standard error confidence intervals, as well as quantitatively using both a feature extraction technique and classification based on a sparse multinomial logistic regression. The results showed that discrimination of inflamed lesions and BCC lesions had a high probability of correct classification. Although classification between the SCC and normal tissue was found prone to error, overall classification accuracy was

95% from all lesions evaluated based on discrimination of inflamed tissue from cancerous tissue. Due to the difficulty in differentiating SCC from normal tissue, further work in this area needs to be pursued, as well as attempts to classify other less common skin abnormalities.

Larraona-Puy et al. investigated the use of Raman spectroscopy to detect and image BCC lesions by developing a spectral-based model derived from tissue excised from 20 patients during Mohs micrographic surgery [46]. In this study, a linear discriminant analysis model was built from the 20 patient database. Spectral features found to provide the greatest separation between the spectra from each representative class were used to classify the blinded tissue samples. The LDA model classified the spectra as BCC, dermis, or epidermis, and the resulting classifications were compared to histopathology. The key differences found between the dermis and BCC were due mainly to contributions from collagen type I spectral features, whereas the main spectral differences between BCC and epidermis correlated to DNA peaks. Not only was the LDA model able to classify BCC from healthy tissue with a high sensitivity and specificity, it was also employed in constructing 2-dimensional biochemical images which correlated strongly with histopathology staining. In a more recent study, Larraona-Puy et al. demonstrated that by using a similar LDA “a priori” model, BCC and hair follicles in skin tissue could be differentiated [47]. Once more, images were constructed and classification was accomplished using this same LDA model. The results showed that differences in DNA and collagen content again provided the high probability of discrimination.

Bodanese and colleagues completed a study in which BCC lesions were differentiated from normal skin tissue by employing a PCA model, as well as a simplified biochemical model based on relative amounts of collagen and fat observed in the Raman spectra [48]. A comparison of the two models showed that the PCA model had a higher specificity and sensitivity than the biochemical model. However, it was noted that the biochemical model has the potential for application to tissues not included in the PCA model, thus providing flexibility by the simple addition of new biochemical spectra. These studies demonstrate the potential Raman spectroscopy has for improving diagnosis of skin cancers, but also the importance of choosing the appropriate model for spectral analysis. Improvement and optimization of classification algorithms and data analysis techniques is an area which needs to be addressed before widespread use of the technique can be applied clinically. Additionally, improvements in the correlation of spectral biomarkers and identification of key spectral regions for identifying cancerous lesions of the skin will also provide improved diagnostic power and detail.

**3.3. Brain Cancer.** Brain cancer accounts for about 2.3% of all cancer related deaths [49]. Gliomas and brain metastases are the most common neoplasms of the brain presented in adults [50]. These malignancies are highly aggressive, and a poor prognosis is given to the majority of patients presenting such conditions [49]. Further complicating the matter, the disease process of the brain is highly complex due to its

intricate neurological structures and unique physiology, and thus results in tumors which are biologically and clinically diverse. This diversity, as well as the infiltration of the tumors into delicate regions of the brain, makes both diagnosis and treatment especially challenging. Early detection is critical to improving a patient's prognosis, although this is often hindered due the initial symptoms having similar characteristics to many other diseases. Surgical excision of brain tumors is the primary method of treatment often requiring tissue samples for histopathological analysis for staging and guiding adjuvant therapy. The most challenging aspect of removing a brain tumor is ensuring tumor margins are clear of all cancerous cells while at the same time minimizing the risk of damage to vital regions of the brain which could cause neurological deficit. Incomplete resection of the cancerous lesion due to imprecise targeting during stereotactic surgery can lead to poor sampling for tissue biopsy as well as a much higher incidence of mortality [50, 51]. Raman spectroscopy could, therefore, potentially provide a means for *in vivo* evaluation of brain tissue and help eliminate unnecessary tissue resection, as well as provide *in situ* tumor margin assessment. Raman spectroscopy may also improve *ex vivo* diagnosis by replacing, or when used in conjunction with, conventional histopathological and immunohistochemical techniques.

Promising results have been demonstrated in the application of Raman spectroscopy for *in vivo* and *ex vivo* diagnostic use in animal models of brain tumors, as well as tissue sections from human biopsies. Previous work by Krafft et al. compared Raman spectroscopy with Fourier transform infrared (FTIR) spectroscopy for the mapping of brain tumors of both mouse and human origin [52, 53]. In a recent investigation by Kirsch and colleagues, a novel proof of concept experiment was performed in that Raman spectroscopy was used to map, *in vivo*, the surface of intercerebral tumors induced in rat brains [54]. A multivariate model based on k-means cluster analysis of the spectra was used to create a false-color map of the surface of the rat brain. The results were compared to hematoxylin- and eosin- (H&E) stained coronal sections of the same area analyzed by Raman spectroscopy. Interestingly, it was observed that the Raman spectroscopic map identified a tumor which was not visible in photomicrographs, as it was below the surface and thus not visually perceptible. Although the penetration depth was only a few hundred microns below the surface, this finding provides evidence that Raman spectroscopy could provide *in situ* tissue evaluation while minimizing the need for tissue excision or biopsy. Further work will need to be done to optimize collection geometry, spatial resolution, and excitation intensity.

In another recent study using an animal model and a microprobe, Beljebbar et al. published findings in which Raman spectroscopy was successfully used to assess C6 glioblastomas implanted in rat brains [51]. Raman spectroscopy was initially used to classify tissue excised from the implanted brain tumors based on a set of reference spectra developed from purified lipids and DNA [51]. The results from the Raman spectra were compared to those from conventional histopathology as the standard for classification.

Principal component analysis (PCA) was performed on the spectra collected with 100% classification accuracy. It was found that decreasing collection times from 100 s to 10 s had little effect on signal averaging, thus providing evidence of a robust approach. To prove the potential for clinical application, implanted tumors were then monitored *in vivo* over a 20-day period using a handheld Raman microprobe. Hierarchical cluster analysis showed a clear separation of spectra collected from normal tissue prior to tumor implantation from spectra taken on days 4 and 20 postimplantation. A strong correlation was also observed between the immunohistochemistry staining and the spectroscopic data from which spectral markers were identified that are associated with proliferative and invasive properties of the tumors. Establishing such spectral biomarkers is of importance as it has been found that biochemical variation between normal and cancerous brain tissue can play a significant role in diagnosis [55].

Raman spectroscopic analysis of lipid extracts from normal brain tissues and malignant brain tumors has demonstrated the ability to determine spectral signatures relating to the concentrations of lipids in the tissues. In particular, the differences in the concentrations of phosphatidylcholine and cholesterol have been observed to be most significant between normal versus cancerous cells [56]. Results from the Raman spectroscopic analysis of the lipid extracts in this study conducted by Köhler et al. were supported by data from highly sensitive mass spectrometry analysis of the same tissue extracts. Another group has focused on using Raman spectroscopy to distinguish between neural crest-derived pediatric tumors [16, 57]. Using freshly resected tissue or biopsies, Raman spectra were collected from tissue samples of 39 patients and analyzed by PCA. A high level of sensitivity and specificity was achieved for classifying and differentiating between neuroblastomas, ganglioneuromas, nerve sheath tumors, pheochromocytomas, and normal adrenal glands [16]. Continued work by the same group showed that the accuracy of classification based on the Raman spectra did not diminish when evaluating cryopreserved tissue while using the model developed from fresh tissue samples [57]. These studies demonstrate the potential Raman spectroscopy has for improving diagnosis and treatment strategies of brain tumors and other related neuropathologies. Surgical procedures involving the excision of brain tumors could benefit greatly from the development of a Raman spectroscopic instrument which could be used for histological evaluation *in situ* and thus limit the risk of damage to the vital neurological structures of the brain. The ability to improve tumor margin clearance based on spectral mapping by use of a handheld Raman probe could also greatly improve prognosis of patients undergoing gross total brain tumor resection.

**3.4. Gastrointestinal Cancers.** Gastrointestinal (GI) cancers include all cancers of the gastrointestinal tract, comprising malignancies of the esophagus, stomach, gallbladder, liver, pancreas, colon, rectum, and anus. Prognosis varies greatly with the type of cancer and the anatomical location in the gastrointestinal tract of the lesion. Patients suffering from

GI cancers are often diagnosed at advanced stages of the disease and thus have poor prognosis and survival rates [58]. Endoscopy, utilizing conventional white-light reflectance, is often used for diagnosis of cancers of the GI tract. However, this method relies on morphological identification of the lesions which can be subject to inaccurate diagnosis, as well as difficulty in diagnosis of early-stage premalignancies and small metastatic sites. As the prognosis of GI cancer patients has been strongly correlated to early diagnosis, the need for a more sensitive diagnostic modality is apparent. Gastric cancer is the second leading cause of cancer-related death worldwide causing an estimated 600,000 deaths annually [59, 60]. Gastric cancer is suspected to be caused by infection by the bacteria *Helicobacter pylori* and increased risk associated with smoking and certain dietary factors. Adenocarcinoma is the most prominent malignancy, presenting approximately 90% of all gastric cancers, of which is subdivided into intestinal and diffuse type.

In previous work, Teh et al. took Raman spectra from 76 gastric tissue samples obtained from 44 patients undergoing investigational endoscopy or gastrectomy [59]. The spectra were analyzed by both PCA-LDA and empirical peak analysis to classify the tissue samples as normal or dysplasia. Conventional histopathology was used as the comparison benchmark, and from this it was observed that the PCA-LDA algorithm yielded a more accurate classification with 90.9% specificity and 95.2% sensitivity. In a later study by the same group, Raman spectroscopy was collected from 100 tissue samples to demonstrate the capability of classifying normal gastric epithelium from the two subtypes of adenocarcinoma, intestinal and diffuse type [60]. Again conventional histopathological evaluation was used as the benchmark. It was observed that significant differences were found between normal stomach tissue and the two adenocarcinoma subtypes. It was also found that by using a combination of PCA and multinomial logistic regression, achievement of high classification accuracy was possible [60].

Raman spectra have been collected from patients, *in vivo*, undergoing endoscopic gastric examination [61–63]. Zheng et al. have developed an image-guided multimodal technique which combines a 785 nm excitation Raman endoscopic probe with a rapid dispersion-type Raman spectrometer, allowing for high-quality spectra to be collected *in vivo* within 0.5 s. The Raman endoscopic imaging system is integrated with white-light reflectance, autofluorescence imaging, and narrow-band imaging capabilities [64]. Furthermore, a custom-designed computer-based control system with data acquisition and analysis, as well as real-time display, allows for both Raman spectra and endoscopic video to be viewed simultaneously. This system is the first of its kind, allowing for clinical evaluation of gastric cancer using Raman spectroscopy combined with the conventional modality of wide-field narrow-band imaging guidance during gastroscopy. This same group has also employed various data mining algorithms for *in situ* spectral analysis for *in vivo* diagnosis of gastric dysplasia and gastric cancers. Linear combination techniques, partial least squares-discriminant analysis, and ant-colony optimization

have all been reported [61–63]. Zheng and colleagues have also recently demonstrated successful application of the multimodal image-guided Raman endoscopy system for *in vivo* diagnosis of esophageal cancer by implementing a highly accurate biomolecular modeling algorithm [65]. The biomolecular model is based on non-negativity-constrained least squares minimization of six biochemical reference spectra of which the significant fit coefficients were fed into an LDA algorithm. The algorithm was able to achieve an accuracy of 96% and define the biomolecules, which are most significant for differentiation amongst the normal and cancerous esophageal mucosa. Furthermore, the same group also completed a study comparing the variability observed in Raman spectra from different regions of the upper GI tract, while also providing characterization of the spectral features of neoplastic lesions in the upper GI tract [66]. This multimodal endoscopic Raman system is one of the mostly highly advanced systems for *in vivo* Raman spectroscopic diagnosis. As improvements in the accuracy of diagnosis and detection are further developed by optimizing data analysis techniques, the potential for Raman spectroscopy in routine clinical use comes closer to reality. This multimodal platform in which Raman spectroscopy is combined with other optical imaging modalities holds promise for clinical application in the near future. As current optics dictate, wide-field imaging can rapidly identify potential areas of interest and Raman spectroscopy can be used to confirm the pathology of those specific areas of interest, providing information based on biomolecular composition and, therefore, diagnosis.

Colorectal cancer is the third most common cause of cancer in men and women worldwide, with over 100,000 cases of colorectal cancer diagnosed in the United States last year alone [67, 68]. Cancer of the colon is much more common than that of the rectum, and while dietary factors are believed to be the most important risk factor for developing colorectal cancer, other factors such as smoking and inflammatory bowel disease are also believed to play a role. Like other gastrointestinal cancers, endoscopy is the primary means of diagnosing colorectal malignancies, and early diagnosis and treatment are strongly related to the patient's prognosis. Prognosis is highly correlated with the degree of tumor penetration through the bowel wall, as well as involvement of the lymph nodes [68]. The asymptomatic nature of colorectal cancer is often attributed to the high level of associated mortality and thus regular screening is essential. As with other GI cancers, detection via endoscopy is subject to the skill and experience of the physician, as well as the characteristics of the lesion. Raman spectroscopy has been investigated for use in an endoscopic role to provide rapid, unambiguous diagnosis of the colorectal malignancies.

Previously, Raman spectra of tissue samples were collected *ex vivo* and classified as normal or malignant using PCA combined with Mahalanobis distance, spectral residuals and a multiparametric limit test. Employing this model, over 99.5% sensitivity and specificity was achieved [69]. Widjaja et al. classified 105 tissue specimens from 59 patients using Raman spectroscopy and applied support vector machines (SVM) for multiclass classification of normal, hyperplastic polyps, and adenocarcinoma [70]. In this study, two types

of SVM (simple and modified) were used in various permutations with three different kernel functions (linear, polynomial, and Gaussian radial basis function (RBF)) to achieve maximum classification accuracy. It was found that conventional SVM combined with RBF kernels obtained an overall diagnostic accuracy of 99.9%. This study demonstrates the power of optimizing data mining techniques when applied to Raman spectroscopy in providing the accuracy of diagnosis necessary to improve clinical outcomes. Beljebbar and colleagues have used Raman spectroscopy of frozen colonic tissue samples to accurately quantify the biochemical compositions and changes associated with adenocarcinoma from normal tissue [71]. Classification of normal and adenocarcinoma tissue samples was achieved by applying and comparing various models based on PCA, cluster analysis and multiple least squares algorithms. Furthermore, spectral features were extracted to construct a robust database which allowed for the generation of pseudocolor Raman maps of the tissue samples. It was shown that the Raman maps correlated well with histopathology staining. Beljebbar and colleagues demonstrate the detailed biochemical understanding Raman spectroscopy can provide and the accurate correlations which can be made between tissue morphology and biomolecular composition. The analysis of such information would allow for not only improved clinical diagnosis but also a better understanding of disease progression, for instance, the process of malignant transformation in large populations of patients.

Esophageal cancer is another gastrointestinal cancer with poor prognosis [72]. Esophageal adenocarcinoma is an aggressive malignancy in which very few patients survive at five years. With 43,700 cases reported in the EU last year, the need for improved diagnosis and treatment is critical [73]. Esophageal adenocarcinoma is caused by the transformation of squamous epithelium of the esophagus to columnar epithelium. This premalignant condition known as Barrett's esophagus is due to reflux disease, which results in a transformation that typically takes several years to progress to high-grade dysplasia or adenocarcinoma. Raman spectroscopy was also shown to have potential in diagnosing esophageal cancer and understanding the biochemical changes associated with esophageal tissue carcinogenesis. Groups have investigated Raman spectroscopy for biochemical mapping of tissues undergoing transformation from Barrett's esophagus to cancerous lesions in an attempt to help better understand the disease mechanism, as well as improve patient survival [74]. Other recent work has focused on developing a miniature confocal fiber-optic Raman probe, which can be used during endoscopic procedures for improved lesion identification in biopsies [75]. The ongoing work in the application of Raman spectroscopy for GI-related malignancies is some of the most promising and advanced work in terms of translation to *in vivo* and clinical applications. The anatomical arrangement of the GI tract and the use of endoscopic image-guided diagnosis, along with the high rate of GI cancer-related mortality, facilitate the highly favorable application of Raman spectroscopy in this area for the near future.

**3.5. Cervical Cancer.** Cervical cancer is the second most common cancer in women worldwide, resulting in approximately 275,000 deaths annually [76]. Persistent infection with the human papillomavirus (HPV) is now understood to be the cause of almost all cases of cervical cancer. Cervical cancer typically develops in the transformational zone of epithelial cells, termed the cervical transformational zone. In this zone, stratified squamous epithelium replaces mucus-producing glandular epithelium; thus again illustrating the significance of cancer-associated potential in such transformational tissue regions [76]. Infection with HPV leads to a much higher risk of cervical dysplasia and is the main risk factor of cervical cancer. As with many other cancers, early detection and diagnosis is key to improving prognosis, particularly with cervical cancer which is highly curable if detected early. Cervical dysplasia is detected by observation of an abnormal Pap smear with subsequent colposcopic examination, biopsy, and histopathological evaluation. The visual histopathological examination of the tissue sections is subject to interobserver variability. Also, early stage malignancy or premalignancy may not be observed due to the limited cytological contribution to the biopsied section. Owing in part to the accessibility of the cervical region, several optical technologies have been investigated for diagnosis with Raman spectroscopy exhibiting particular promise [77].

Several studies using *in-vitro* cultures have shown encouraging results for the application of Raman spectroscopy for improving the detection and screening of cervical cancer as well as investigating the biochemical changes associated with HPV infection [78, 79]. Lyng et al. investigated tissue samples from 40 patients using Raman spectroscopy, and a PCA-LDA model to classify the samples as normal, cervical intraepithelial neoplasia (pre-malignant) or invasive carcinoma [80]. In a study by Vidyasagar et al., Raman spectra were collected from the cervical tissues of patients undergoing radiotherapy for treatment of cervical cancer [81]. This study found that Raman spectroscopy could accurately predict tumor response to the radiotherapy treatment based on unsupervised and supervised classification techniques.

Recently, several *in vivo* studies have been performed in which a portable Raman spectroscopic fiber-probe system was utilized for diagnosis of cervical abnormalities. In a follow-up study from previous work, Robichaux-Viehoever et al. collected Raman spectra from the cervix of 79 patients *in vivo* using a clinically relevant spectra collection time of 5 s [82]. Normal spectra were collected from patients undergoing hysterectomy (normal cervical tissue), and spectra correlating to cervical dysplasia were collected from patients with abnormal Pap smears. The spectra were classified based on corresponding histopathological evaluation into five categories (normal ectocervix, normal endocervix, squamous metaplasia, low-grade dysplasia, high-grade dysplasia). Several logistic regression discrimination algorithms were constructed for classification of the five histopathological groups and an independent data set served to validate the models. It was found that Raman spectroscopy achieved a higher sensitivity and specificity for classification of

high-grade dysplasia from benign tissue samples than by colposcopic examination. Optimization of the algorithm, including development of separate algorithms for each pathological grouping, may improve the accuracy further. As this is an on-going study, the increasing patient population will improve modeling efforts and should provide a model which can classify tissues in a manner superior to current clinical methodology. Kanter et al. performed another study demonstrating the potential Raman spectroscopy has for detecting subtle variations in both cervical dysplasia and normal cervical tissues due to hormonal effects caused by menopause and the menstruation cycle [83]. The study aimed to improve classification of the most difficult pathology to correctly classify low-grade squamous intraepithelial lesions (LGSIL), which are often misclassified as normal tissue. Using a two-step data analysis technique based on a diagnostic feature extraction step, followed by a probabilistic classification scheme, spectra from 122 patients were classified with significantly improved accuracy. Stratification of the data into separate classes based on menstrual cycle phase allowed for the classification accuracy of LGSIL to improve from 74% to 97%. Raman spectroscopy has the potential to become a highly sensitive tool for detecting and accurately classifying cervical abnormalities while greatly reducing the need for biopsies and the associated morbidity.

**3.6. Oral Cancer.** Oral and pharyngeal cancer, combined, make up the sixth most common cancer in the world, with over 50% of diagnosed cases proving fatal [84]. The most important risk factors are tobacco use and excessive alcohol intake, which have been attributed to more than 80% of all cases [85]. As has been observed with many other cancers, presentation of late stages of the disease is common due to lack of diagnosis and thus results in a poor prognosis for the patient. Oral and oropharynx cancers are found with a disproportionately higher incidence among impoverished populations [86]. Cancers of the oral cavity, including oral squamous cell carcinomas (OSCC), oral leukoplakia (OLK), and premalignant lesions, are most often diagnosed by visual inspection of the oral cavity [87]. Several recently published studies have evaluated Raman spectroscopy as a potential new method for early diagnosis of OSCC [88, 89]. Li et al. demonstrated the use of near-infrared FTIR spectroscopy in tandem with support vector machines for classifying OSCC, OLK, and normal tissues [90]. Using FTIR and SVM, Li et al. were able to achieve a high level of sensitivity, specificity, and accuracy; therefore, Raman spectroscopy may also have the potential to provide similar, if not superior, results. The ease of access to the oral cavity and pharynx also provides promise for the use of Raman spectroscopy in the detection of oral cancer, especially when combined with wide-field or autofluorescence imaging technologies. Recent literature on the use of Raman spectroscopy for oral cancer diagnosis has been sparse, particularly for conventional dispersive Raman spectroscopy, although there is potential for the technology to improve early diagnosis and supplement or even replace conventional techniques.

**3.7. Lung Cancer.** Lung cancer has a higher level of mortality than breast, prostate, and colorectal cancers combined, making it the leading cause of cancer-related death worldwide [91–93]. Tobacco smoking is the leading risk factor for lung cancer, although the disease is found in nonsmokers as well. A majority of lung cancer-related deaths, an estimated 64%, occurred in developing countries in 2008 [94]. Lung cancer has a poor prognosis, as it is often diagnosed at a late stage, contributing to the high level mortality with average five-year survival of approximately 15% [95]. Early detection is difficult due to the asymptomatic nature of lung cancer, particularly due to the prevalence of the disease in the elder population in which early symptoms may often be attributed to comorbidities related to other health conditions. Preliminary diagnosis and early detection has most often been carried out by chest X-ray, as well as sputum cytology, and more recently low-dose radiation computed tomography (LDCT) or spiral computer tomography [96]. More invasive diagnosis which may be able to identify the type of cancer present often includes bronchoscopy, fine-needle aspiration with ultra sound guidance, or CT-guided biopsy. Conventional histopathological examination of biopsied tissue is used to classify lung cancers. Lung cancers most commonly arise from epithelial tissues of the lung resulting in malignant carcinomas. Four distinct histological types of lung carcinoma have been defined: small-cell carcinoma, squamous-cell carcinoma, adenocarcinoma, and large-cell carcinoma [97]. The latter three are often grouped into what is commonly referred to as nonsmall cell carcinoma; accounting for approximately 85% of all lung cancers [98]. Prognosis and treatment are dictated by histological classification, and accurate staging is critical to providing the appropriate treatment. The high degree of heterogeneity observed in lung cancer complicates the classification and therefore can affect staging, treatment, and ultimately patient outcome [99]. Furthermore, it has been found that the accuracy of histological diagnosis based on the examination of biopsy is unacceptably low due to subjective error from interobserver variability [100–102]. For example, in 2008 it was observed in the UK that the average rate of correct histological confirmation was 73%; with a range of 88% to as low as 25% correct histological confirmation [102]. Thus, due to the complexity in classifying biopsies containing multiple cell types combined with the variance in histopathological evaluation, Raman spectroscopy may hold a great deal of potential for improving diagnosis and staging of lung cancer.

Raman spectroscopy has recently been investigated by several groups for a wide variety of applications in the diagnosis and classification of lung cancers. Magee et al. used Raman spectroscopy to analyze induced sputum for the detection of molecular profiles associated with lung cancer based on distinguishing healthy, and “at-risk” subjects from those with confirmed lung cancer [103]. The group of “at-risk” subjects was classified as having one or more risk factors for lung cancer, such as being a smoker. Raman spectroscopy demonstrated the ability to differentiate sputum of lung cancer patients from “at-risk” subjects with 90% sensitivity and 60% specificity, while “at-risk” subjects

were differentiated from healthy control subjects with 90% sensitivity and 93% specificity. This study demonstrates the unique molecular signatures which Raman spectroscopy is capable of detecting and thus distinguishing, which could prove beneficial as a noninvasive, rapid screening modality. Using Raman spectroscopy in such a fashion could provide an initial screening method prior to the use of more invasive or expensive modalities such as LDCT. The same group has also demonstrated that Raman spectroscopy may have the capability to predict early postoperative recurrence of lung cancer. Spectral indicators may show a relation of elevated levels of DNA and reduced levels of porphyrin in the tumor tissue compared to that of normal lung tissue [104].

Raman spectroscopy has also been applied in tandem with FTIR to demonstrate the potential such a bimodal system could have for diagnosis and biochemical analysis of lung cancer [105–107]. Krafft et al. have demonstrated success in combining both Raman and FTIR to evaluate congenital cystic adenomatoid malformations (CCAMs) [106, 107]. Raman maps of the *ex vivo* CCAM tissue specimens were developed by implementing multiplicative signal correction and k-means cluster analysis. The data analysis procedure was optimized so that artifacts observed in Raman and FTIR spectra were minimized and thus the combination of the two vibrational spectroscopic techniques became complimentary [106]. Both high- and low-resolution analyses were performed demonstrating the flexibility Raman spectroscopy can provide by identifying the differences in both cellular and biochemical compositions via control over the lateral resolution [107]. Such resolution control was not possible with FTIR. In an effort to move Raman spectroscopy to *in vivo* clinical applications, several groups have focused on developing an optimized endoscopic probe for bronchoscopic diagnosis of lung cancer [108, 109]. Short et al. have shown that adding Raman spectroscopy to current white light bronchoscopy/autofluorescence bronchoscopy (WFB/AFB) improves sensitivity and specificity for the detection of preneoplastic lesions *in vivo* [110]. Short and colleagues combined all three modalities to demonstrate *in vivo* detection of preneoplastic lesions in 26 patients. Using PCA-LDA and fitting of a combination biomolecular models, they were able to obtain a sensitivity of 96% and a specificity of 91%. Although these studies show the improvements Raman spectroscopy could provide in the diagnosis and staging of lung cancer, continued work is needed to develop an optimized probe and data analysis model for this trimodal application. Additional work is being done to identify disease specific biomarkers from Raman spectra which correlate to biochemical signatures of specific histological signs of malignancy [111].

#### **4. Future Developments towards Clinical Applications of Raman Spectroscopy**

Surgery is the front line of defense for the treatment of many cancers. Current intraoperative assessment of suspect tissue or demarcation of tumor margins has relied on conventional histopathological analysis of biopsied tissue or physical

inspection based on preoperative images. Such techniques have inherent levels of subjectivity and are prone to inter-observer variability. Often these conventional techniques can prove unreliable for the detection of microscopic or premalignant lesions which then results in delayed diagnosis and additional surgery. Furthermore, biopsy of tissue has associated morbidity, and in some cases the removal of tissue for investigative purposes is too high a risk due to the involved vital anatomy. Even when tissue is biopsied, typically small sections are actually surveyed and serve to represent a much larger area which can result in misdiagnosis. Raman spectroscopy provides an objective technique for biopsy evaluation, which is based on molecular composition of the tissue using advanced algorithms. For diseases in which the associated risk and comorbidity of biopsy is low or tissue excision is required, Raman spectroscopy has the potential to provide a detailed evaluation, and classification of tissue *ex vivo* based on the biochemical composition. Raman spectroscopy could be used in conjunction with current histopathology and immunohistochemistry, and in the future could replace these techniques with a significantly more rapid, cost-effective analysis technique. Numerous proof-of-concept studies have demonstrated successful results using a standard microscope-based platform and current spectral analysis algorithms which have shown sensitivities, specificities, and accuracies which are greater than or equal to that of the conventional histopathological assessment. Continued advancements in data mining techniques for Raman spectroscopy will allow for extraction and classification of spectral details from data sets of incredible size using super computers [112, 113]. Raman spectroscopy has been shown to have potential to improve diagnosis of a great number of diseases, including many of the most prevalent and fatal cancers.

Continued collection of spectral data from tissues could allow for a spectral library to be built which could then be investigated as improved data extraction and analysis methods are developed. As some studies have already shown, this data can be used to track and understand disease progression which could lead to improved treatments and disease models [114]. Due to the large amount of information contained in Raman spectra collected from tissues, a continued focus of research should be placed on data mining to optimize the information extraction. Correlation of spectral features and changes associated with progression of disease could provide a wealth of information concerning disease-specific biochemical markers related to differences between normal and various stages of cancer development. Such information could be further correlated with other biological and nonbiological patient factors for disease risk assessment of large patient populations. Focus on the elucidation of disease-specific spectral biomarkers, with the assignment of spectral signatures to differences observed on the cellular level, could lead to a determinant for selecting personalized therapies for each patient.

The application of techniques such as surface-enhanced Raman spectroscopy (SERS) could help greatly improve such personalized treatments by targeting cells with highly

specific antibodies and tunable optical performance capabilities [115–117]. SERS allows for the enhancement of the Raman signal up to 10–15 orders of magnitude depending upon the SERS substrate and the Raman system used. This phenomenon is attributed to the localized surface plasmon which occurs on nanodimensionally roughened surfaces or nanoparticles which are often made of gold, silver, and recently carbon nanotubes [118–120]. In order for the Raman spectroscopic signal to become enhanced, the localized surface plasmon must be confined to a small region on the substrate surface, thus nanoparticles or nanofabricated surfaces are optimal SERS substrates for developing highly specific, targeted molecular imaging and detection capabilities for biological environments [119, 120]. Gold nanoparticles have demonstrated application as highly effective SERS probes as they exhibit low toxicity, are capable of being functionalized with antibodies for targeting, provide multimodal imaging contrast enhancement, as well as potential therapeutic effects by laser ablation methods [121–123]. The optical tunability of the SERS particles based on the particles' radius, shape, and morphology, as well as the tagging of particles with cell-specific antibodies provides a highly advantageous technique for diagnosing cancer on the molecular level and providing more effective targeted therapies [124, 125]. Recently, *in vivo* studies by Keren et al. have demonstrated successful targeting and deep-tissue molecular imaging with SERS-active nanoparticles and carbon nanotubes [126]. *In vivo* work such as this will help set the stage for future applications of highly targeted cancer detection and therapy utilizing Raman spectroscopy in tandem with the rapidly progressing field of nanotechnology.

*In vivo* applications of Raman spectroscopy for solid organs and hollow cavities of the body will require improvements in different areas of technology, even as many promising preliminary results have been presented. Table 2 summarizes the recent studies which have involved the *in vivo* applications of Raman spectroscopy for cancer diagnosis. Designing a probe which can be inserted into endoscopic channels will allow for convenient investigation of hollow organs such as the colon, esophagus, and stomach as well as less invasive access to the surfaces of solid organs [127]. For intraoperative investigation of cancerous lesions such as for the demarcation of tumor margins or *in situ* staging, an optimized flexible fiber-optic-based probe will need to be developed. This fiber-optic probe must have ideal optical properties and capable of being produced relatively cheaply. Thus far, development of a fiber-optic Raman probe for endoscopic use has been difficult due to the spectral interference of fused silica fibers in the fingerprint region of 400–2000  $\text{cm}^{-1}$  [128]. The background signal of the silica fibers, in the 700–1300  $\text{cm}^{-1}$  range, has plagued the design and development of a clinically viable *in vivo* probe as the background obliterates the weak Raman signal from the sample. Also, most commercially available probes are too large (>10 mm diameter) for insertion into endoscopic channels; therefore, probes with diameters of 2 mm or less must be developed with high signal-to-noise ratios (SNR) while capable of rapid spectra acquisition times of only a few seconds [129]. The continued innovations

in spectrometer components such as CCD detectors have allowed for improved spectral acquisition times, but even with the development of high-grade low-OH silica fibers the background noise generated by the fibers remains. However, in light of this hurdle, a number of groups have been working on developing such a fiber-optic Raman spectroscopic probe system, including some encouraging clinical results [110, 111, 130, 131].

Fiber-optic Raman probes are generally based on confocal type design or micro- (or miniaturized) fiber-optic Raman probe design [127]. Confocal designs are larger in diameter, although they are more effective at removing fiber-generated scatter and fluorescence as the configuration of optics is less limited by size constraints. In the micro-Raman probe design, all optical components (lenses, filters) are fitted to the tip of probe in a highly compact construction. Various aspects of probe design have been under development including decreasing the probe diameter while maintaining optical purity and lowering SNR [131]. A 600  $\mu\text{m}$  diameter micro-Raman probe was recently developed by Komachi and colleagues with high-quality optical fibers and a collecting lens with incorporated filters at the tip of the probe [132]. The narrow probes designed by Komachi et al. have a circular arrangement of collection fibers around a central excitation fiber of which the diameter is related to the focal length of the probe. The collection efficiency of the probe was increased from the original design by attaching a bandpass filter at the tip of the excitation fiber and a long pass filter at the tip of the collection fiber ring. Using this probe design, Raman spectra from skin were measured (5 s acquisition time, 40 mW excitation) yielding high collection efficiency and high SNR. This type of probe design has the potential to be used for intravascular applications as well due to the small diameter of the probe. Day et al. present the design of a miniature confocal Raman probe using anisotropic wet-etching methods typically used for fabricating silicon wafers for computer motherboards [133]. The miniature confocal probe was shown to achieve similar spectral collection capabilities as those of a conventional microscope at the same power and with collection times of several seconds. This confocal Raman probe was designed for endoscopic use and was demonstrated *ex vivo* in the pathological evaluation of potentially cancerous lesions of surgically resected esophageal tissue. Importantly these studies are prime examples of the innovations needed for realizing *in vivo* applications of Raman spectroscopy, particularly related to the need for a fiber-optic Raman probe.

Monte Carlo models have been employed to calculate depth-dependent sensitivity and sampling volume in relation to lens geometry, refractive index, absorption, and scattering coefficients for variations of fiber configuration [129, 134]. The Monte Carlo models are important in predicting the variability of spectral contributions based on sampling volumes. This is particularly true for the analysis of epithelial tissues where tissue is layered and such spatial distributions should be accounted for when assessing cancerous tissues based on Raman spectra [134]. Mo et al. demonstrated how changes in the refractive index and diameter of the ball-lens

TABLE 2: A summary of the recent *in vivo* applications of Raman spectroscopy for cancer diagnosis discussed in the present paper. Type of cancer, number of patients (and/or number of spectra if reported), data analysis methods, and diagnostic outcome are presented for each reference. The studies utilizing the rat model for brain cancer are presented in this table, although these were not human clinical trials, for comparison with the state of current technology.

Type of cancer	Number of patients	Data analysis	Outcome	Reference
Breast	9 (31 spectra acquired)	Fitting of spectra based on linear combination model coefficients from <i>ex vivo</i> tissue samples	Sensitivity: 100% Specificity: 100% Accuracy: 93.3%	[31]
Skin	19 (21 tissue sites with total of 42 spectra)	Nonlinear maximum representation and discrimination (MRDF) and Sparse linear multinomial logistic regression (SMLR)	Sensitivity: 100% Specificity: 91% Accuracy: 95%	[45]
Brain	Rat model (C6 glioma cells for glioblastoma model)	Principial component analysis (PCA), Ward's Clustering algorithm and square Euclidian distance measures	<i>In vivo</i> classification based on <i>ex vivo</i> model with 100% accuracy	[51]
Brain	Rat model (cortical and subcortical melanotic tumor model)	k-means cluster analysis	Development of false-color tissue map of brain tumors;tumor margins delineated	[54]
Gastric*	67 (238 total tissue sites)	Nonnegative constrained least squares minimization with Classification and Regression Tree (CART) model	Sensitivity: 94.0% Specificity: 93.4% Accuracy: 93.7%	[61]
Gastric*	71 (1102 spectra acquired)	Partial least squares and linear discriminant analysis (PLS-DA)	Sensitivities: 93.8, 84.7, 82.1% Specificities: 93.8, 94.5, 95.3% (normal, benign, malignant)	[62]
Gastric*	67 (238 total tissue sites)	Ant colony optimization integrated with linear discriminant analysis (ACO-LDA)	Sensitivity: 94.6%, 89.3% Specificity: 94.6%, 97.8% Accuracy: 94.6%, 96.7% (diagnostic, predictive)	[63]
Esophageal	27 (75 total tissue sites)	Nonnegative constrained least squares minimization (NNCLSM) and linear discriminate analysis (LDA)	Sensitivity: 97.0% Specificity: 95.2% Accuracy: 96.0%	[65]
Upper GI tract	107 (1189 spectra acquired)	Nonnegative constrained least squares minimization (NNCLSM) with reference database for biomolecular modeling	Sensitivities: 92.6%, 90.9% Specificities: 88.6%, 93.9% Accuracy: 89.3%, 94.7% (gastric, esophagus)	[66]
Cervical	66* (172 tissue sites) (11 patients excluded)	Logistic regression discrimination algorithms	Sensitivity: 89% Specificity: 81%	[82]
Cervical (effect of hormonal variation on cervical disease)	122	Nonlinear maximum representation and discrimination (MRDF) and Sparse linear multinomial logistic regression (SMLR)	Incorporation of the hormonal variation information into a previous model improved model accuracy from 74% to 97% for diagnosis of LGSIL	[83]
Lung	26 (129 spectra acquired)	Principal component analysis and linear discriminant analysis with a databased biomolecular model	Sensitivity: 96% Specificity: 91%	[110]

\* Denotes that these three studies involved the same group of patients.

can provide depth-resolved Raman measurements in a two-layer epithelial tissue model [130]. Not only should the probe design be considered, but the design of the entire Raman system must be optimized for the use of the probe; as collection efficiency is correlated with coupling of the probe to the spectrometer [132]. Other optical fiber probe designs have been investigated, such as the hollow optical fibers [127]. Matsuura et al. have used hollow glass tubes with silver-coated waveguides to develop a flexible probe capable of excitation and collection of Raman-scattered photons [135,

136]. Although hollow waveguides circumvent the spectral interference caused by fused silica fibers they are expensive and complicated to manufacture. High wavenumber Raman spectroscopy (HWNRS) is another modality of Raman spectroscopy that may allow for some of the obstacles with conventional fiber-optic probe design to be circumvented. High-wavenumber refers to the spectral region of 2500–4000  $\text{cm}^{-1}$ . This region does not suffer from the background signal and fluorescence created by fused silica fibers and thus may be suited for the development of a simpler fiber-optic

Raman probe without the need for complex filters. HWNRS also can allow for commercially available endoscopic probes to be utilized. A few recent studies have demonstrated successful application of HWNRS for the detection of various cancers, including breast and cervical cancer [137, 138]. Although HWNRS has the advantage of highly reduced fiber background signal, this region of the spectra lacks a great deal of spectral features found in the fingerprint region. Water also has a broad band in this region of the Raman spectrum.

For applications involving Raman spectroscopic tissue mapping, scan times of the area of interest need to be reduced to a clinically acceptable timeframe. Point-by-point mapping is the typical method for creating a 2-dimensional Raman spectral map. This is done by moving in a stepwise manner across a sample, also known as rastering, refocusing the laser each time, and then collecting the spectra of each point over a defined range of the spectrum which is then translated into a 2-dimensional map [139]. Each pixel of the map will correlate to an  $x$ - $y$  coordinate on the sample. Although this method allows for very high resolution maps to be created, even with motorized stages this procedure leads to long mapping times (up to several hours or more), which are not feasible for the clinical use. Raman spectroscopic tissue mapping has applications in histopathological analysis of biopsies *ex vivo*, as well as potential for mapping tissue *in vivo*, such as for tissue analysis and whole tumor localization and demarcation. For such applications to be realized and put to use in the clinical setting much more rapid acquisition times are necessary. Line scanning illumination is a method which has recently been shown capable of collecting spectra from a line of up to 1 mm in length. Line scanning allows for 100 or more spectra to be collected simultaneously and thus reducing scan time and power density at the sample surface dramatically [140]. Line scanning is possible due to the introduction of the intermediate slit in the spectrometer and the geometry of illumination of the CCD detector. Global illumination, or true imaging, is another method which can be used to reduce mapping times [139, 140]. Global illumination uses a series, or wheel, of tunable filters which are selected for specific Raman bands of interest. This technique allows for very rapid collection of spectra over relatively large areas, although the density of information collected is sacrificed. A comprehensive comparison of the three methods of point-by-point, line scanning and wide-field imaging is provided by Schlücker et al. [141]. More recent applications have used a defocused beam to improve upon the global illumination technique. Future applications of Raman spectroscopy to solid organs and tissue surfaces, particularly with regards to 3-dimensional Raman imaging or deep-tissue analysis, will require improvements in the penetration depth as well as higher spatial resolution in both the lateral and axial directions. Matousek and Stone review several of the deep Raman spectroscopic techniques which may allow for the development of truly noninvasive Raman scattering-based modalities for cancer detection and imaging of organs and tissues deep within the body [142]. Further developments of deep Raman spectroscopic techniques could allow for tissues and organs to be viewed in great detail, including 3-dimensional maps based on biochemical and

cellular distributions. Additionally, combinations of other modalities with Raman spectroscopy such as hyperspectral imaging, or more conventional imaging modalities such MRI may also be on the horizon.

## 5. Conclusion

Cancer remains one of the most common causes of death, as well as one of the most demanding burdens on healthcare systems throughout the world. In the recent years, research interests have focused on optical spectroscopic techniques for the diagnosis of cancer and from this Raman spectroscopy has received considerable attention. Numerous studies from the laboratory bench-top to the clinical bedside have produced encouraging results; however, additional advancements in Raman spectroscopy are needed before such clinical applications become realized. Continued development of Raman spectroscopic instrumentation is needed to perform at the level necessary for clinical use, including the design of a complete hardware apparatus which is compact and can be easily integrated into the clinical setting. Optimization of algorithms and the development of software interfaces which are automated and simplified for use by clinicians and surgical staff without the need for extensive training also must be developed fully. Many technical challenges must be overcome by innovative research before Raman spectroscopy can become a standard clinical tool. In spite of this, the growing interest in the field and innovations in optics, electronics and data mining affords a promising outlook into the future for clinical applications in cancer detection and diagnosis.

## Acknowledgments

This paper is partially supported by a UF Research Opportunity Fund (2011-2012) and the Center for Applied Optimization.

## References

- [1] F. K. Tangka, J. G. Trogon, and L. C. Richardson, "Cancer treatment cost in the United States: has the burden shifted over time?" *Cancer*, vol. 116, no. 14, pp. 3477–3484, 2010.
- [2] A. Jemal, R. Siegel, J. Xu, and E. Ward, "Cancer statistics, 2010," *CA Cancer Journal for Clinicians*, vol. 60, no. 5, pp. 277–300, 2010.
- [3] S. Keereweer, J. D. F. Kerrebijn, and P. B. A. A. van Driel, "Optical image-guided surgery—where do we stand?" *Molecular Imaging and Biology*, vol. 13, no. 2, pp. 199–207, 2011.
- [4] C. A. Owen, I. Notingher, R. Hill, M. Stevens, and L. L. Hench, "Progress in Raman spectroscopy in the fields of tissue engineering, diagnostics and toxicological testing," *Journal of Materials Science*, vol. 17, no. 11, pp. 1019–1023, 2006.
- [5] J. J. Blaker, J. E. Gough, V. Maquet, I. Notingher, and A. R. Boccacini, "In vitro evaluation of novel bioactive composites based on Bioglass-filled polylactide foams for bone tissue engineering scaffolds," *Journal of Biomedical Materials Research*, vol. 67, no. 4, pp. 1401–1411, 2003.

- [6] S. Wachsmann-Hogiu, T. Weeks, and T. Huser, "Chemical analysis in vivo and in vitro by Raman spectroscopy—from single cells to humans," *Current Opinion in Biotechnology*, vol. 20, no. 1, pp. 63–73, 2009.
- [7] I. Notingher, S. Verrier, S. Haque, J. M. Polak, and L. L. Hench, "Spectroscopic study of human lung epithelial cells (A549) in culture: living cells versus dead cells," *Biopolymers*, vol. 72, no. 4, pp. 230–240, 2003.
- [8] G. Pyrgiotakis, O. E. Kundakcioglu, P. M. Pardalos et al., "Raman spectroscopy and support vector machines for quick toxicological evaluation of titania nanoparticles," *Journal of Raman Spectroscopy*, vol. 42, no. 6, pp. 1222–1231, 2011.
- [9] G. Pyrgiotakis, O. E. Kundakcioglu, K. Finton, P. M. Pardalos, K. Powers, and B. M. Moudgil, "Cell death discrimination with raman spectroscopy and support vector machines," *Annals of Biomedical Engineering*, vol. 37, no. 7, pp. 1464–1473, 2009.
- [10] I. Notingher, C. Green, C. Dyer et al., "Discrimination between ricin and sulphur mustard toxicity *in vitro* using Raman spectroscopy," *Journal of the Royal Society Interface*, vol. 1, no. 1, pp. 79–90, 2004.
- [11] C. H. Arnaud, "Raman heads for the clinic," *Chemical and Engineering News*, vol. 88, no. 38, pp. 8–12, 2010.
- [12] N. Stone and C. A. Kendall, "Raman spectroscopy for early cancer detection, diagnosis and elucidation of disease-specific biochemical changes," in *Emerging Raman Applications and Techniques in Biomedical and Pharmaceutical Fields*, M. Pavel and M. D. Morris, Eds., chapter 13, pp. 315–346, Springer, Berlin, Germany, 2010.
- [13] S. Wold, K. Esbensen, and P. Geladi, "Principal component analysis," *Chemometrics and Intelligent Laboratory Systems*, vol. 2, no. 1–3, pp. 37–52, 1987.
- [14] P. A. Lachenbruch and M. Goldstein, "Discriminant analysis," *Biometrics*, vol. 35, no. 1, pp. 69–85, 1979.
- [15] N. Cristianini and J. Shawe-Taylor, Eds., *An Introduction to Support Vector Machines—and other Kernel-Based Learning Methods*, Cambridge University Press, Cambridge, UK, 2005.
- [16] R. Rabah, R. Weber, G. K. Serhatkulu et al., "Diagnosis of neuroblastoma and ganglioneuroma using Raman spectroscopy," *Journal of Pediatric Surgery*, vol. 43, no. 1, pp. 171–176, 2008.
- [17] J. Horsnell, P. Stonelake, J. Christie-Brown et al., "Raman spectroscopy—a new method for the intra-operative assessment of axillary lymph nodes," *Analyst*, vol. 135, no. 12, pp. 3042–3047, 2010.
- [18] M. Sattlecker, C. Bessant, J. Smith, and N. Stone, "Investigation of support vector machines and Raman spectroscopy for lymph node diagnostics," *Analyst*, vol. 135, no. 5, pp. 895–901, 2010.
- [19] J. W. Chan, D. S. Taylor, and S. M. Lane, "Nondestructive identification of individual leukemia cells by laser trapping raman spectroscopy," *Analytical Chemistry*, vol. 80, no. 6, pp. 2180–2187, 2008.
- [20] M. S. Bergholt, W. Zheng, K. Lin et al., "Combining near-infrared-excited autofluorescence and Raman spectroscopy improves *in vivo* diagnosis of gastric cancer," *Biosensors and Bioelectronics*, vol. 26, no. 10, pp. 4104–4110, 2011.
- [21] J. H. Ward, "Hierarchical grouping to optimise an objective function," *Journal of the American Statistical Association*, vol. 58, pp. 236–244, 1963.
- [22] A. S. Hartigan and M. A. Wong, "A k-means clustering algorithm," *Journal of the Royal Society of Statistical Society*, vol. 28, no. 1, pp. 100–108, 1979.
- [23] K. Meister, D. A. Schmidt, and E. Bründermann, "Confocal Raman microspectroscopy as an analytical tool to assess the mitochondrial status in human spermatozoa," *Analyst*, vol. 135, no. 6, pp. 1370–1374, 2010.
- [24] F. Draux, P. Jeannesson, A. Beljebbar et al., "Raman spectral imaging of single living cancer cells: a preliminary study," *Analyst*, vol. 134, no. 3, pp. 542–548, 2009.
- [25] R. Kohavi, "A study of cross-validation and bootstrap for accuracy estimation and model selection," in *Proceedings of the 14th International Joint Conference on Artificial Intelligence*, vol. 2, pp. 1137–1143, 1995.
- [26] V. N. Vapnik, *The Nature of Statistical Learning Theory*, Springer, 2000.
- [27] V. N. Vapnik and V. Vapnik, *Statistical Learning Theory*, vol. 2, Wiley, New York, NY, USA, 1998.
- [28] American Cancer Society, *Breast Cancer Facts & Figures 2009–2010*, American Cancer Society, Atlanta, Ga, USA.
- [29] H. G. Welch, S. Woloshin, and L. M. Schwartz, "The sea of uncertainty surrounding ductal carcinoma in situ—the price of screening mammography," *Journal of the National Cancer Institute*, vol. 100, no. 4, pp. 228–229, 2008.
- [30] A. S. Haka, K. E. Shafer-Peltier, M. Fitzmaurice, J. Crowe, R. R. Dasari, and M. S. Feld, "Diagnosing breast cancer by using Raman spectroscopy," *Proceedings of the National Academy of Sciences of the United States of America*, vol. 102, no. 35, pp. 12371–12376, 2005.
- [31] A. S. Haka, Z. Volynskaya, J. A. Gardecki et al., "In vivo margin assessment during partial mastectomy breast surgery using Raman spectroscopy," *Cancer Research*, vol. 66, no. 6, pp. 3317–3322, 2006.
- [32] A. S. Haka, Z. Volynskaya, J. A. Gardecki et al., "Diagnosing breast cancer using Raman spectroscopy: prospective analysis," *Journal of Biomedical Optics*, vol. 14, no. 5, p. 054023, 2009.
- [33] M. V. P. Chowdary, K. Kumar, J. Kurien, S. Mathew, and C. M. Krishna, "Discrimination of normal, benign, and malignant breast tissues by Raman spectroscopy," *Biopolymers*, vol. 83, no. 5, pp. 556–569, 2006.
- [34] K. K. Kumar, M. V. P. Chowdary, S. Mathew, L. Rao, C. M. Krishna, and J. Kurien, "Raman spectroscopic diagnosis of breast cancers: evaluation of models," *Journal of Raman Spectroscopy*, vol. 39, no. 9, pp. 1276–1282, 2008.
- [35] American Cancer Society, *Breast Cancer: Treatment Guidelines for Patients*, American Cancer Society, Atlanta, Ga, USA, 2005.
- [36] S. Rehman, Z. Movasaghi, A. T. Tucker et al., "Raman spectroscopic analysis of breast cancer tissues: identifying differences between normal, invasive ductal carcinoma and ductal carcinoma in situ of the breast tissue," *Journal of Raman Spectroscopy*, vol. 38, no. 10, pp. 1345–1351, 2007.
- [37] H. Silberman and A. Silberman, Eds., *Principles and Practice of Surgical Oncology*, Lippincott Williams and Wilkins, Philadelphia, Pa, USA, 2010.
- [38] H. Abramczyk, J. Surmacki, B. Brozek-Pluska, Z. Morawiec, and M. Tazbir, "The hallmarks of breast cancer by Raman spectroscopy," *Journal of Molecular Structure*, vol. 924–926, no. C, pp. 175–182, 2009.
- [39] L. Wheless, J. Black, and A. J. Alberg, "Nonmelanoma skin cancer and the risk of second primary cancers: a systematic review," *Cancer Epidemiology Biomarkers and Prevention*, vol. 19, no. 7, pp. 1686–1695, 2010.
- [40] A. F. Jerant, J. T. Johnson, C. D. Sheridan, and T. J. Caffrey, "Early detection and treatment of skin cancer," *American Family Physician*, vol. 62, no. 2, pp. 357–368, 2000.

- [41] J. D. Whited and J. M. Grichnik, "Does this patient have a mole or a melanoma?" *Journal of the American Medical Association*, vol. 279, no. 9, pp. 696–701, 1998.
- [42] D. L. Shriner, D. K. McCoy, D. J. Goldberg, and R. F. Wagner, "Mohs micrographic surgery," *Journal of the American Academy of Dermatology*, vol. 39, no. 1, pp. 79–97, 1998.
- [43] R. M. Levy and C. W. Hanke, "Mohs micrographic surgery: facts and controversies," *Clinics in Dermatology*, vol. 28, no. 3, pp. 269–274, 2010.
- [44] L. Brochez, E. Verhaeghe, E. Grosshans et al., "Inter-observer variation in the histopathological diagnosis of clinically suspicious pigmented skin lesions," *The Journal of Pathology*, vol. 196, no. 4, pp. 459–466, 2002.
- [45] C. A. Lieber, S. K. Majumder, D. L. Ellis, D. D. Billheimer, and A. Mahadevan-Jansen, "In vivo nonmelanoma skin cancer diagnosis using Raman microspectroscopy," *Lasers in Surgery and Medicine*, vol. 40, no. 7, pp. 461–467, 2008.
- [46] M. Larraona-Puy, A. Ghita, A. Zoladek et al., "Development of Raman microspectroscopy for automated detection and imaging of basal cell carcinoma," *Journal of Biomedical Optics*, vol. 14, no. 5, Article ID 054031, 2009.
- [47] M. Larraona-Puy, A. Ghita, A. Zoladek et al., "Discrimination between basal cell carcinoma and hair follicles in skin tissue sections by Raman micro-spectroscopy," *Journal of Molecular Structure*, vol. 993, no. 1–3, pp. 57–61, 2011.
- [48] B. Bodanese, L. Silveira, R. Albertini, R. A. Zângaro, and M. T. T. Pacheco, "Differentiating normal and basal cell carcinoma human skin tissues *in vitro* using dispersive Raman spectroscopy: a comparison between principal components analysis and simplified biochemical models," *Photomedicine and Laser Surgery*, vol. 28, supplement 1, pp. S119–S127, 2010.
- [49] R. El-Zein, M. Bondy, and M. Wrensch, "Brain tumors," in *Epidemiology of Brain Tumors*, F. Ali-Osman, Ed., chapter 1, Humana Press, Totowas, NJ, USA, 2005.
- [50] M. Mut and D. Schiff, "Unmet needs in the treatment of glioblastoma," *Expert Review of Anticancer Therapy*, vol. 9, no. 5, pp. 545–551, 2009.
- [51] A. Beljebbar, S. Dukic, N. Amharref, and M. Manfait, "Ex vivo and in vivo diagnosis of C6 glioblastoma development by Raman spectroscopy coupled to a microprobe," *Analytical and Bioanalytical Chemistry*, vol. 398, no. 1, pp. 477–487, 2010.
- [52] C. Krafft, S. B. Sobottka, G. Schackert, and R. Salzer, "Raman and infrared spectroscopic mapping of human primary intracranial tumors: a comparative study," *Journal of Raman Spectroscopy*, vol. 37, no. 1–3, pp. 367–375, 2006.
- [53] C. Krafft, M. Kirsch, C. Beletes, G. Schackert, and R. Salzer, "Methodology for fiber-optic Raman mapping and FTIR imaging of metastases in mouse brains," *Analytical and Bioanalytical Chemistry*, vol. 389, no. 4, pp. 1133–1142, 2007.
- [54] M. Kirsch, G. Schackert, R. Salzer, and C. Krafft, "Raman spectroscopic imaging for in vivo detection of cerebral brain metastases," *Analytical and Bioanalytical Chemistry*, vol. 398, no. 4, pp. 1707–1713, 2010.
- [55] D. I. Ellis and R. Goodacre, "Metabolic fingerprinting in disease diagnosis: biomedical applications of infrared and Raman spectroscopy," *Analyst*, vol. 131, no. 8, pp. 875–885, 2006.
- [56] M. Köhler, S. MacHill, R. Salzer, and C. Krafft, "Characterization of lipid extracts from brain tissue and tumors using Raman spectroscopy and mass spectrometry," *Analytical and Bioanalytical Chemistry*, vol. 393, no. 5, pp. 1513–1520, 2009.
- [57] H. Wills, R. Kast, C. Stewart et al., "Raman spectroscopy detects and distinguishes neuroblastoma and related tissues in fresh and (banked) frozen specimens," *Journal of Pediatric Surgery*, vol. 44, no. 2, pp. 386–391, 2009.
- [58] A. Okines, M. Verheij, W. Allum, D. Cunningham, and A. Cervantes, "Gastric cancer: ESMO clinical practice guidelines for diagnosis, treatment and follow-up," *Annals of Oncology*, vol. 21, no. 5, pp. v50–v54, 2010.
- [59] S. K. Teh, W. Zheng, K. Y. Ho, M. Teh, K. G. Yeoh, and Z. Huang, "Diagnostic potential of near-infrared Raman spectroscopy in the stomach: differentiating dysplasia from normal tissue," *British Journal of Cancer*, vol. 98, no. 2, pp. 457–465, 2008.
- [60] S. K. Teh, W. Zheng, K. Y. Ho, M. Teh, K. G. Yeoh, and Z. Huang, "Near-infrared Raman spectroscopy for early diagnosis and typing of adenocarcinoma in the stomach," *British Journal of Surgery*, vol. 97, no. 4, pp. 550–557, 2010.
- [61] Z. Huang, S. K. Teh, W. Zheng et al., "In vivo detection of epithelial neoplasia in the stomach using image-guided Raman endoscopy," *Biosensors and Bioelectronics*, vol. 26, no. 2, pp. 383–389, 2010.
- [62] M. S. Bergholt, W. Zheng, K. Lin et al., "Raman endoscopy for *in vivo* differentiation between benign and malignant ulcers in the stomach," *Analyst*, vol. 135, no. 12, pp. 3162–3168, 2010.
- [63] M. S. Bergholt, W. Zheng, K. Lin et al., "In vivo diagnosis of gastric cancer using Raman endoscopy and ant colony optimization techniques," *International Journal of Cancer*, vol. 128, no. 11, pp. 2673–2680, 2011.
- [64] M. S. Bergholt, W. Zheng, K. Lin et al., "Combining near-infrared-excited autofluorescence and Raman spectroscopy improves *in vivo* diagnosis of gastric cancer," *Biosensors and Bioelectronics*, vol. 26, no. 10, pp. 4104–4110, 2011.
- [65] M. S. Bergholt, W. Zheng, K. Lin et al., "In vivo diagnosis of esophageal cancer using image-guided Raman endoscopy and biomolecular modeling," *Technology in Cancer Research and Treatment*, vol. 10, no. 2, pp. 103–112, 2011.
- [66] M. S. Bergholt, W. Zheng, K. Lin et al., "Characterizing variability in *in vivo* Raman spectra of different anatomical locations in the upper gastrointestinal tract toward cancer detection," *Journal of Biomedical Optics*, vol. 16, no. 3, Article ID 037003, 2011.
- [67] A. Jemal, R. Siegel, Y. Hao et al., "Cancer statistics, 2008," *CA Cancer Journal for Clinicians*, vol. 58, no. 2, pp. 71–96, 2008.
- [68] R. Labianca, B. Nordlinger, G. D. Beretta, A. Brouquet, and A. Cervantes, "Primary colon cancer: ESMO clinical practice guidelines for diagnosis, adjuvant treatment and follow-up," *Annals of Oncology*, vol. 21, supplement 5, pp. v70–v77, 2010.
- [69] M. V. Chowdary, K. K. Kumar, K. Thakur et al., "Discrimination of normal and malignant mucosal tissues of the colon by Raman spectroscopy," *Photomedicine and Laser Surgery*, vol. 25, no. 4, pp. 269–274, 2007.
- [70] E. Widjaja, W. Zheng, and Z. Huang, "Classification of colonic tissues using near-infrared Raman spectroscopy and support vector machines," *International Journal of Oncology*, vol. 32, no. 3, pp. 653–662, 2008.
- [71] A. Beljebbar, O. Bouché, M. D. Diébold et al., "Identification of Raman spectroscopic markers for the characterization of normal and adenocarcinomatous colonic tissues," *Critical Reviews in Oncology/Hematology*, vol. 72, no. 3, pp. 255–264, 2009.
- [72] K. K. Wang and R. E. Sampliner, "Updated guidelines 2008 for the diagnosis, surveillance and therapy of Barrett's

- esophagus," *American Journal of Gastroenterology*, vol. 103, no. 3, pp. 788–797, 2008.
- [73] M. Stahl, W. Budach, H. J. Meyer, and A. Cervantes, "Esophageal cancer: clinical practice guidelines for diagnosis, treatment and follow-up," *Annals of Oncology*, vol. 21, supplement 5, pp. v46–v49, 2010.
- [74] G. Shetty, C. Kendall, N. Shepherd, N. Stone, and H. Barr, "Raman spectroscopy: elucidation of biochemical changes in carcinogenesis of oesophagus," *British Journal of Cancer*, vol. 94, no. 10, pp. 1460–1464, 2006.
- [75] C. Kendall, J. Day, J. Hutchings et al., "Evaluation of Raman probe for oesophageal cancer diagnostics," *Analyst*, vol. 135, no. 12, pp. 3038–3041, 2010.
- [76] M. Schiffman, P. E. Castle, J. Jeronimo, A. C. Rodriguez, and S. Wacholder, "Human papillomavirus and cervical cancer," *The Lancet*, vol. 370, no. 9590, pp. 890–907, 2007.
- [77] C. M. Krishna, G. D. Sockalingum, and M. S. Vidyasagar, "An overview on applications of optical spectroscopy in cervical cancers," *Journal of Cancer Research and Therapeutics*, vol. 4, no. 1, pp. 26–36, 2008.
- [78] P. R. T. Jess, D. D. W. Smith, M. Mazilu, K. Dholakia, A. C. Riches, and C. S. Herrington, "Early detection of cervical neoplasia by Raman spectroscopy," *International Journal of Cancer*, vol. 121, no. 12, pp. 2723–2728, 2007.
- [79] K. M. Ostrowska, A. Malkin, A. Meade et al., "Investigation of the influence of high-risk human papillomavirus on the biochemical composition of cervical cancer cells using vibrational spectroscopy," *Analyst*, vol. 135, no. 12, pp. 3087–3093, 2010.
- [80] F. M. Lyng, E. Ó. Faoláin, J. Conroy et al., "Vibrational spectroscopy for cervical cancer pathology, from biochemical analysis to diagnostic tool," *Experimental and Molecular Pathology*, vol. 82, no. 2, pp. 121–129, 2007.
- [81] M. S. Vidyasagar, K. Maheedhar, B. M. Vadhiraja, D. J. Fernandes, V. B. Kartha, and C. M. Krishna, "Prediction of radiotherapy response in cervix cancer by Raman spectroscopy: a pilot study," *Biopolymers*, vol. 89, no. 6, pp. 530–537, 2008.
- [82] A. Robichaux-Viehoever, E. Kanter, H. Shappell, D. Billheimer, H. Jones, and A. Mahadevan-Jansen, "Characterization of Raman spectra measured *in vivo* for the detection of cervical dysplasia," *Applied Spectroscopy*, vol. 61, no. 9, pp. 986–993, 2007.
- [83] E. M. Kanter, S. Majumder, G. J. Kanter, E. M. Woeste, and A. Mahadevan-Jansen, "Effect of hormonal variation on Raman spectra for cervical disease detection," *American Journal of Obstetrics and Gynecology*, vol. 200, no. 5, pp. 512.e1–512.e5, 2009.
- [84] S. Warnakulasuriya, "Global epidemiology of oral and oropharyngeal cancer," *Oral Oncology*, vol. 45, no. 4-5, pp. 309–316, 2009.
- [85] S. Warnakulasuriya, "Living with oral cancer: epidemiology with particular reference to prevalence and life-style changes that influence survival," *Oral Oncology*, vol. 46, no. 6, pp. 407–410, 2010.
- [86] N. W. Johnson, S. Warnakulasuriya, P. C. Gupta et al., "Global oral health inequalities in incidence and outcomes for oral cancer: causes and solutions," *Advances in Dental Research*, vol. 23, no. 2, pp. 237–246, 2011.
- [87] C. Scully, J. S. Bagan, C. Hopper, and J. B. Epstein, "Oral cancer: current and future diagnostic techniques," *American Journal of Dentistry*, vol. 21, no. 4, pp. 199–209, 2008.
- [88] C. M. Krishna, G. D. Sockalingum, J. Kurien et al., "Micro-Raman spectroscopy for optical pathology of oral squamous cell carcinoma," *Applied Spectroscopy*, vol. 58, no. 9, pp. 1128–1135, 2004.
- [89] R. Malini, K. Venkatakrishna, J. Kurien et al., "Discrimination of normal, inflammatory, premalignant, and malignant oral tissue: a Raman spectroscopy study," *Biopolymers*, vol. 81, no. 3, pp. 179–193, 2006.
- [90] Y. Li, Z. Wen, L. Li, M. L. Li, N. Gao, and Y. Z. Guo, "Research on the Raman spectral character and diagnostic value of squamous cell carcinoma of oral mucosa," *Journal of Raman Spectroscopy*, vol. 41, no. 2, pp. 142–147, 2010.
- [91] C. N. Klabunde, P. M. Marcus, G. A. Silvestri et al., "U.S. primary care physicians' lung cancer screening beliefs and recommendations," *American Journal of Preventive Medicine*, vol. 39, no. 5, pp. 411–420, 2010.
- [92] C. M. Tammemagi, P. F. Pinsky, N. E. Caporaso et al., "Lung cancer risk prediction: prostate, lung, colorectal and ovarian cancer screening trial models and validation," *Journal of the National Cancer Institute*, vol. 103, no. 13, pp. 1058–1068, 2011.
- [93] D. R. Brenner, J. R. McLaughlin, and R. J. Hung, "Previous lung diseases and lung cancer risk: a systemic review and meta-analysis," *PLoS One*, vol. 6, no. 3, article e17479, 2011.
- [94] A. Jemal, F. Bray, M. M. Center, J. Ferlay, E. Ward, and D. Forman, "Global cancer statistics," *CA Cancer Journal for Clinicians*, vol. 61, no. 2, pp. 69–90, 2011.
- [95] L. G. Collins, C. Haines, R. Perkel, and R. E. Enck, "Lung cancer: diagnosis and management," *American Family Physician*, vol. 75, no. 1, pp. 56–63, 2007.
- [96] P. B. Bach, M. J. Kelley, R. C. Tate, and D. C. McCrory, "Screening for lung cancer: a review of the current literature," *Chest*, vol. 123, supplement 1, pp. 72S–82S, 2003.
- [97] J. E. Tyczynski, F. Bray, and D. M. Parkin, "Lung cancer in Europe in 2000: epidemiology, prevention, and early detection," *The Lancet Oncology*, vol. 4, no. 1, pp. 45–55, 2003.
- [98] J. R. Molina, P. Yang, S. D. Cassivi, S. E. Schild, and A. A. Adjei, "Non-small cell lung cancer: epidemiology, risk factors, treatment, and survivorship," *Mayo Clinic Proceedings*, vol. 83, no. 5, pp. 584–594, 2008.
- [99] V. L. Roggli, R. T. Vollmer, S. D. Greenberg et al., "Lung cancer heterogeneity: a blinded and randomized study of 100 consecutive cases," *Human Pathology*, vol. 16, no. 6, pp. 569–579, 1985.
- [100] R. W. Field, B. J. Smith, C. E. Platz et al., "Lung cancer histologic type in the surveillance, epidemiology, and end results registry versus independent review," *Journal of the National Cancer Institute*, vol. 96, no. 14, pp. 1105–1107, 2004.
- [101] J. S. Thomas, D. Lamb, T. Ashcroft et al., "How reliable is the diagnosis of lung cancer using small biopsy specimens? Report of a UKCCCR Lung Cancer Working Party," *Thorax*, vol. 48, no. 11, pp. 1135–1139, 1993.
- [102] R. Booton, F. Blackhall, and K. Kerr, "Individualised treatment in non-small cell lung cancer: precise tissue diagnosis for all?" *Thorax*, vol. 66, no. 4, pp. 273–275, 2011.
- [103] N. D. Magee, R. J. Beattie, R. Gray et al., "Raman spectroscopy analysis of induced sputum in lung cancer," *American Journal of Respiratory and Critical Care Medicine*, vol. 181, Article ID A3492, 2010.
- [104] N. D. Magee, M. Ennis, J. S. Elborn et al., "Raman microscopy in the diagnosis and prognosis of surgically resected non-small cell lung cancer," *Journal of Biomedical Optics*, vol. 15, no. 2, Article ID 026015, 2010.

- [105] J. Lv, L. Zhang, J. Feng et al., "Optical observation of lung cancer with attenuated total reflectance-fourier transform infrared microscope (ATR-FTIR) and confocal Raman microscope," *Spectroscopy Letters*, vol. 44, no. 5, pp. 312–317, 2011.
- [106] C. Krafft, D. Codrich, G. Pelizzo, and V. Sergo, "Raman and FTIR imaging of lung tissue: methodology for control samples," *Vibrational Spectroscopy*, vol. 46, no. 2, pp. 141–149, 2008.
- [107] C. Krafft, D. Codrich, G. Pelizzo, and V. Sergo, "Raman mapping and FTIR imaging of lung tissue: congenital cystic adenomatoid malformation," *Analyst*, vol. 133, no. 3, pp. 361–371, 2008.
- [108] N. D. Magee, J. S. Villaumie, E. T. Marple, M. Ennis, J. S. Elborn, and J. J. McGarvey, "Ex vivo diagnosis of lung cancer using a Raman miniprobe," *Journal of Physical Chemistry B*, vol. 113, no. 23, pp. 8137–8141, 2009.
- [109] M. A. Short, S. Lam, A. McWilliams, J. Zhao, H. Lui, and H. Zeng, "Development and preliminary results of an endoscopic Raman probe for potential *in vivo* diagnosis of lung cancers," *Optics Letters*, vol. 33, no. 7, pp. 711–713, 2008.
- [110] M. A. Short, S. Lam, A. M. McWilliams, D. N. Ionescu, and H. Zeng, "Using laser raman spectroscopy to reduce false positives of autofluorescence bronchoscopies: a pilot study," *Journal of Thoracic Oncology*, vol. 6, no. 7, pp. 1206–1214, 2011.
- [111] P. Xanthopoulos, R. De Asmundis, M. R. Guarracino, G. Pyrgiotakis, and P. M. Pardalos, "Supervised classification methods for mining cell differences as depicted by Raman spectroscopy," in *Computational Intelligence Methods for Bioinformatics and Biostatistics*, R. Rizzo and P. J. G. Lisboa, Eds., Lecture Notes in Bioinformatics, pp. 112–122, Springer, 2011.
- [112] M. Guarracino, P. Xanthopoulos, G. Pyrgiotakis et al., "Classification of cancer cell death with spectral dimensionality reduction and generalized eigenvalues," *Artificial Intelligence in Medicine*, vol. 53, no. 2, pp. 119–125, 2011.
- [113] Y. Oshima, H. Shinzawa, T. Takenaka, C. Furihata, and H. Sato, "Discrimination analysis of human lung cancer cells associated with histological type and malignancy using Raman spectroscopy," *Journal of Biomedical Optics*, vol. 15, no. 1, p. 017009, 2010.
- [114] C. Kendall, J. Hutchings, H. Barr, N. Shepherd, and N. Stone, "Exploiting the diagnostic potential of biomolecular fingerprinting with vibrational spectroscopy," *Faraday Discussions*, vol. 149, pp. 279–290, 2011.
- [115] X. M. Qian and S. M. Nie, "Single-molecule and single-nanoparticle SERS: from fundamental mechanisms to biomedical applications," *Chemical Society Reviews*, vol. 37, no. 5, pp. 912–920, 2008.
- [116] J. H. Kim, J. S. Kim, H. Choi et al., "Nanoparticle probes with surface enhanced Raman spectroscopic tags for cellular cancer targeting," *Analytical Chemistry*, vol. 78, no. 19, pp. 6967–6973, 2006.
- [117] T. Vo-Dinh, H. N. Wang, and J. Scaffidi, "Plasmonic nanoprobe for SERS biosensing and bioimaging," *Journal of Biophotonics*, vol. 3, no. 1-2, pp. 89–102, 2010.
- [118] A. Champion and P. Kambhampati, "Surface-enhanced Raman scattering," *Chemical Society Reviews*, vol. 27, no. 4, pp. 241–250, 1998.
- [119] A. W. Wark, R. J. Stokes, S. B. Darby, W. E. Smith, and D. Graham, "Dynamic imaging analysis of SERS-active nanoparticle clusters in suspension," *Journal of Physical Chemistry C*, vol. 114, no. 42, pp. 18115–18120, 2010.
- [120] C. Zavaleta, A. Zerda, Z. Liu et al., "Noninvasive Raman spectroscopy in living mice for evaluation of tumor targeting with carbon nanotubes," *Nano Letters*, vol. 8, no. 9, pp. 2800–2805, 2008.
- [121] W. Xie, P. Qiu, and C. Mao, "Bio-imaging, detection and analysis by using nanostructures as SERS substrates," *Journal of Materials Chemistry*, vol. 21, no. 14, pp. 5190–5202, 2011.
- [122] W. Cai, T. Gao, H. Hong, Sun, and S. Jiangtao, "Applications of gold nanoparticles in cancer nanotechnology," *Nanotechnology, Science and Applications*, vol. 1, pp. 17–32, 2008.
- [123] G. von Maltzahn, A. Centrone, J. H. Park et al., "SERS-coded cold nanorods as a multifunctional platform for densely multiplexed near-infrared imaging and photothermal heating," *Advanced Materials*, vol. 21, no. 31, pp. 3175–3180, 2009.
- [124] M. Sha, H. Xu, S. G. Penn, and R. Cromer, "SERS nanoparticles: a new optical detection modality for cancer diagnosis," *Nanomedicine*, vol. 2, no. 5, pp. 725–734, 2007.
- [125] N. Guarrotxena and G. C. Bazan, "Antibody-functionalized SERS tags with improved sensitivity," *Chemical Communications*, vol. 47, no. 31, pp. 8784–8786, 2011.
- [126] S. Keren, C. Zavaleta, Z. Cheng, A. De La Zerda, O. Gheysens, and S. S. Gambhir, "Noninvasive molecular imaging of small living subjects using Raman spectroscopy," *Proceedings of the National Academy of Sciences of the United States of America*, vol. 105, no. 15, pp. 5844–5849, 2008.
- [127] H. Sato, H. Shinzawa, and Y. Komachi, "Fiber-optic Raman probes for biomedical and pharmaceutical applications," in *Emerging Raman Applications and Techniques in Biomedical and Pharmaceutical Fields*, M. Pavel and M. D. Morris, Eds., chapter 2, Springer, Berlin, Germany, 2010.
- [128] A. Nijssen, S. Koljenovic, T. C. Bakker Schut, P. J. Caspers, and G. J. Puppels, "Towards oncological application of Raman spectroscopy," *Journal of Biophotonics*, vol. 2, no. 1-2, pp. 29–36, 2009.
- [129] J. T. Motz, M. Hunter, L. H. Galindo et al., "Optical fiber probe for biomedical Raman spectroscopy," *Applied Optics*, vol. 43, no. 3, pp. 542–554, 2004.
- [130] J. Mo, W. Zheng, and Z. Huang, "Fiber-optic probe couples ball lens for depth-selected Raman measurements of epithelial tissues," *Biomedical Optics Express*, vol. 1, pp. 17–30, 2010.
- [131] Z. Huang, S. K. Teh, W. Zheng et al., "Integrated Raman spectroscopy and trimodal wide-field imaging techniques for real-time *in vivo* tissue Raman measurements at endoscopy," *Optics Letters*, vol. 34, no. 6, pp. 758–760, 2009.
- [132] Y. Komachi, T. Katagiri, H. Sato, and H. Tashiro, "Improvement and analysis of a micro Raman probe," *Applied Optics*, vol. 48, no. 9, pp. 1683–1696, 2009.
- [133] J. C. C. Day, R. Bennett, B. Smith et al., "A miniature confocal Raman probe for endoscopic use," *Physics in Medicine and Biology*, vol. 54, no. 23, pp. 7077–7087, 2009.
- [134] C. Reble, I. Gersonde, C. A. Lieber, and J. Helfmann, "Influence of tissue absorption and scattering on depth dependent sensitivity of Raman fiber probe investigated by Monte Carlo simulations," *Biomedical Optics Express*, vol. 2, no. 3, pp. 520–532, 2011.
- [135] Y. Komachi, S. Hidetoshi, Y. Matsuura, M. Miyagi, and H. Tashiro, "Raman probe using a single hollow waveguide," *Optics Letters*, vol. 30, no. 21, pp. 2942–2944, 2005.
- [136] Y. Matsuura, S. Kino, E. Yokoyama, T. Katagiri, H. Sato, and H. Tashiro, "Flexible fiber-optics probes for Raman and FT-IR remote spectroscopy," *IEEE Journal on Selected Topics in Quantum Electronics*, vol. 13, no. 6, pp. 1704–1708, 2007.
- [137] J. Mo, W. Zheng, J. J. H. Low, J. Ng, A. Ilancheran, and Z. Huang, "High wavenumber raman spectroscopy for *in vivo*

- detection of cervical dysplasia,” *Analytical Chemistry*, vol. 81, no. 21, pp. 8908–8915, 2009.
- [138] A. F. García-Flores, L. Raniero, R. A. Canevari et al., “High-wavenumber FT-Raman spectroscopy for in vivo and ex vivo measurements of breast cancer,” *Theoretical Chemistry Accounts*. In press.
- [139] F. W. L. Esmonde-White and M. D. Morris, “Raman imaging and Raman mapping,” in *Emerging Raman Applications and Techniques in Biomedical and Pharmaceutical Fields*, M. Pavel and M. D. Morris, Eds., chapter 5, Springer, Berlin, Germany, 2010.
- [140] G. D. Pitt, D. N. Batchelder, R. Bennett et al., “Engineering aspects and applications of the new Raman instrumentation,” *IEE Proceedings*, vol. 152, no. 6, pp. 241–318, 2005.
- [141] S. Schlücker, M. D. Schaeberle, S. W. Huffman, and I. W. Levin, “Raman microspectroscopy: a comparison of point, line, and wide-field imaging methodologies,” *Analytical Chemistry*, vol. 75, no. 16, pp. 4312–4318, 2003.
- [142] P. Matousek and N. Stone, “Emerging concepts in deep Raman spectroscopy of biological tissue,” *Analyst*, vol. 134, no. 6, pp. 1058–1066, 2009.

